DYNAMIC TIDAL POWER (DTP): A REVIEW OF A PROMISING TECHNIQUE FOR HARVESTING SUSTAINABLE ENERGY AT SEA

From	: Harmen Talstra, Tom Pak (Svašek Hydraulics)
To	: ir. W.L. Walraven (Stichting DTP Netherlands)
Date	: 29 July 2020
Reference	: 2037/U20232/A/HTAL
Checked by	: A.J. Bliek
Status	: Draft on behalf of whitepaper

1 INTRODUCTION

This memorandum describes the technique of Dynamic Tidal Power (DTP), a conceptually new way of harvesting large-scale tidal energy at open sea; in particular we focus upon the hydrodynamic aspects of it.

At present, most existing installations exploiting tidal energy encompass a structure at the mouth of a river, estuary or tidal basin. This rather small scale limits the amount of sustainable energy that can be extracted, whereas these type of exploitations may cause conflicts with other (e.g. economical or ecological) functions of vulnerable coastal or estuarine waters. The concept of DTP includes a truly large-scale sustainable energy production by utilizing the tidal wave propagation at open sea. This can be done by creating a water head difference over a (very) long dike, roughly perpendicular to the local tidal flow direction, taking advantage of the oscillatory dynamic behaviour of tidal waves. These dikes can be considered as long sequences of pre-fab solid dike modules, containing a large concentration of energy turbines. Dikes can be either attached to an existing coast line, or be constructed at a detached “stand-alone” location at open sea (for instance in combination with an offshore wind farm). The presence of such long dikes at open sea can possibly be utilized for additional economical and environmental functionalities as well.

The presence of long DTP dikes will obviously have a great impact on over-all tidal hydrodynamics at sea (certainly at the continental shelf). Meanwhile, the concept of Dynamic Tidal Power may yield a reliable baseload, which may account for a great part of sustainable energy needed on-shore. Furthermore, its functionality on a daily basis is virtually guaranteed (due to the permanent presence of tidal influence on earth) and its demand for energy storage may be low compared to wind and solar energy (at least if power output fluctuations due to the spring tide / neap tide cycle are accepted). In spite of these advantages, it is obvious that the hydrodynamic and environmental impact of DTP structures at open sea can have an enormous scope and must be subject of thorough study and political debate before actual construction.

This memorandum addresses the following topics:

- A description of the fundamental physical concept behind Dynamic Tidal Power, and a brief review of existing literature regarding DTP and its hydrodynamics;
- A review of the applicability of such idealized descriptions of DTP hydrodynamics for practical cases, especially in relatively shallow coastal seas. Do such schematized cases add value above a full numerical model?
- Numerical calculations of DTP configurations along the Dutch North Sea coast, performed by Svašek Hydraulics (2019) as an estimate for the practical effectiveness of DTP;
- Finally, a brief overview of some hydrodynamic and morphological difficulties that may be encountered when constructing a real DTP dike in a North Sea-like environment, as well as other practical and political aspects of DTP.

2 BASIC PRINCIPLES OF DTP

The essential physical principle of Dynamic Tidal Power (DTP) can be described as well as imagined in a rather simple way (see also Figure 1): when a periodic tidal flow at open sea is partially blocked by means of a long dike perpendicular to the main tidal flow direction, the surrounding water mass will be forced to alternately decelerate and accelerate around the dike at the same pace in which the tidal flow changes direction. This gives rise to alternating zones of water level set-up and set-down on both sides of the structure, and hence a periodic water level difference (which also exerts a net periodic force on the dike).

It is vital that the ambient flow is periodic, and that inertia effects dominate above other dynamic effects, like drag; especially the inertia and acceleration/deceleration of periodic flow is able to induce a considerable head difference across the dike (of the order of magnitude of the tidal range), whereas the blockage of a virtually steady or quasi-steady flow could only induce a head difference of the order of the velocity height (typically a few cm's).

If the constructed perpendicular dike contains a sequence of energy turbines, the head difference will induce a flow discharge through these turbines which can be exploited to harvest electrical energy over the full dike length. The design characteristics of such turbines not only determine their energy efficiency, but also the relation between head difference and discharge (Q-H curve). This Q-H relation implies that, generally, the presence of turbines will give rise to a decrease in head difference (as the DTP dike is in fact partially opened). When designing of a DTP installation, an optimal trade-off needs to be sought between "sufficient turbine flow discharge" and "not too much loss of water level difference" in order to determine the optimal turbine concentration along DTP dikes. It is also possible to extend the active DTP dike by means of additional "bars" (without turbines, either perpendicular to the DTP dike or angled) in order to improve its performance.

The above basic principles of DTP have been introduced and explained by Hulsbergen et al. in various conference publications (2005, 2008). A very accessible quantitative introduction of these principles has been elaborated by Bitter (2018) in a study by Antea Group.

Essentially, this basic DTP principle is often explained using the simple case of a linear and uniform "longshore" tidal wave in a frictionless sea of constant depth, without any site-specific geographical or geophysical information. Various contributions made by Chiang C. Mei (2012, 2019, 2020), partially based upon earlier work by Buchwald (1971, 1974), study the influence of tidal diffraction (which may be important in the case of long DTP dikes) and introduce the effect of the earth's rotation (Coriolis force). In many coastal seas (on the continental shelf) a so-called Kelvin wave can be found: i.e. a wave in the ocean (or atmosphere) that balances the earth's Coriolis force against a topographic boundary such as a coastline. In this way, the Coriolis effect induces a pattern of amphidromic points (tidal nodes), surrounded by a tidal waves with enhanced amplitude that propagate longshore. The presence of such Kelvin waves can make DTP dikes attached to a coastline more attractive than "free" DTP dikes at open sea, because the maximum tidal range in coastal seas is often found near-shore.

Still, the extended analysis by Mei (2012, 2019, 2020) uses many idealizing assumptions: constant bathymetry, a monochromatic tide, absence of bottom friction and convective flow non-linearities, and the absence of irregular coastlines; also, the effect of drag forces on the DTP dikes is often not modeled. One can therefore safely state that in 100% of the practical cases the effect of DTP installations on tidal flow, head differences and energy production should be examined by means of a suitable numerical model. A number of explorative studies have been performed to examine the potential of the DTP technique for various coastal regions around the world: e.g. the Yellow Sea (Hulsbergen et al., 2008, 2012), Orkney Islands (Lemmens, 2017), Bangladesh (Ali et al., 2012 and Roy et al., 2015), Taiwan Strait (Liu and Zhang, 2014), New Brunswick (Gaia Project, 2014) and the North Sea (Svašek Hydraulics, this study). All of these studies apply a form of numerical analysis.

3 IDEALIZATIONS OF DTP HYDRODYNAMICS AND THEIR APPLICABILITY

In this section, we examine and verify more closely the basic principle of DTP as quantified by Hulsbergen (2005, 2008) and Bitter (2018), in order to assess the applicability of an idealized description of DTP hydrodynamics for practical cases. This will be done by simulating the occurring head difference over DTP dams of various types in a schematized rectangular sea with uniform tidal motion, using the computational flow model FINEL, and compare it with the basic formulation for the maximum head difference as given by Hulsbergen (2005, 2008), Bitter (2018) and Mei (2012, 2019).

FINEL is a numerical 2D or 3D parallel flow model developed and maintained by Svašek Hydraulics, based on the Finite Element Method (FEM); it is originally based on research work by Labeur (2009) and Labeur & Wells (2012) on efficient finite element flow solvers. The model can be used either in 3D mode (solving the full hydrostatic or non-hydrostatic Navier-Stokes Equations) of in 2D depth-averaged fashion (solving the Shallow Water Equations). FINEL employs a flexible mesh of triangles or tetrahedra, which enable the user to conveniently incorporate complex coastlines and other boundaries in a model set-up. FINEL can deal with flow over weirs and barriers, drying-/wetting events and many other physical processes and boundary conditions. In the present study the 2D depth-averaged mode of FINEL is employed, which is convenient for the present case of long tidal waves in a shallow sea of constant density.

We consider a rectangular sea of length 2000 km and width 1000 km in case of a detached open-sea DTP dike (or width 500 km in case of a coast-attached DTP dike, see Figure 1), with uniform depth 30 m and a uniform tidal wave travelling from left to right. For convenience, we take a uniform harmonic S_2 tide with variable amplitude and a wave period of 12.0 h.

The mathematical background of the derivation of the maximum head difference over a straight DTP dam is briefly discussed here; for a full elaboration, see the authors mentioned at the start of this section. Bitter (2018) explains how the water mass surrounding a DTP dike will be forced to alternately decelerate and accelerate around the dike at given tidal frequency; this case is said to be equivalent to the case of a thin DTP plate which moves periodically through a surrounding water mass at rest. For dikes that are (much) shorter than the tidal wave length (to avoid diffraction effects), the net resulting tidal force on the DTP dike (as a function of time) can be expressed in the following way:

$$F(t) = m_a dV/dt + \frac{1}{2} C_d \rho V(t)^2 S \qquad (1)$$

in which:

$F(t)$ Net resulting tidal force on DTP dike (as a function of time)

$V(t)$ Undisturbed tidal velocity (as a function of time)

m_a The mass of the water body that is forced to decelerate and accelerate against the DTP dike (the so-called “added mass”);

C_d Drag coefficient;

ρ Density of sea water (which can be taken constant as ρ = 1025 kg/m^3 in this study);

S The “wet surface” of the DTP dike (basically dam length times water depth).

In fact, this equation is fully equivalent to Morison’s Equation (see Det Norske Veritas, 2010), which is widely applied in offshore situations to calculate wave loads on slender cylindrical piles (like foundations for offshore wind turbines) for which diffraction does not play a role. In Eq. (1), the first right-hand-side term (containing added mass and flow acceleration) describes the inertia force whereas the second term accounts for the drag force. The relative importance of both terms is described by the Keulegan-Carpenter number (KC), expressing the ratio of drag over inertia:

$$KC = V_{max}T/L \qquad (2)$$

in which :

KC Dimensionless Keulegan-Carpenter number;

V_{max} Undisturbed tidal velocity amplitude;

T The tidal wave period (e.g. 12.0 h for S_2 tide and 12.4 h for M_2 tide);

L A representative length scale of the dike. (As will turn out later, it is convenient to take L as being the full dike length for DTP dikes attached to a coast, and as being half of the dike length in case of a separate open-sea DTP dike. In this way, the KC number of both dikes will be fully equivalent; see also Figure 1.)

For $KC \gg 1$ the drag force will dominate, whereas for KC values of the order ≈ 1 or smaller the inertia force will be the most important effect; for DTP dams of at least several tens of km's length, the latter will often be the case. In this case the drag force term can be dropped, reducing Equation (1) to the convenient form $F(t) = m_a dV/dt$. As explained by Bitter (2018), the near-dike region that contains the "added mass" has the form of a circle in case of an open-sea DTP dike (and a semi-circle in case of a coastal DTP dike), with radius L. This has been illustrated in Figure 1 below, simultaneously for the case of an open-sea dike and a coast-attached dike. It is important to note that the net force against the DTP dike is proportional to tidal *acceleration*, not velocity (!).

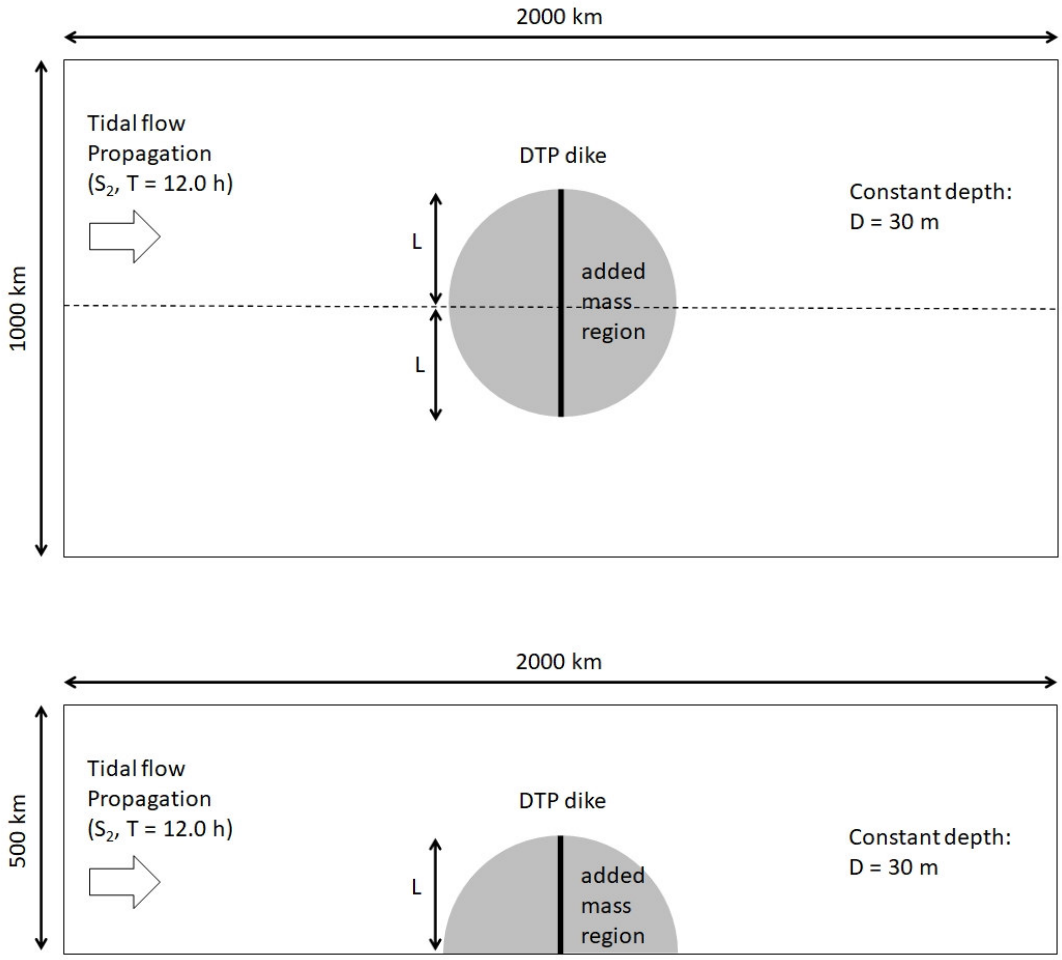

*Figure 1: Lay-out of a straight DTP dike in a schematized rectangular sea with uniform depth and uniform harmonic S_2 tidal wave, with the circular "added mass" region around the DTP dike indicated in light gray. Upper panel: detached open-sea DTP dike with length 2*L, lower panel: coast-attached DTP dike with length L.*

Along a simple straight DTP dike without any extensions, the head difference amplitude over the dike follows an approximate elliptic pattern (see Bitter, 2018 and Mei, 2019); it reaches its maximum half-way the open-sea dam (or right a the coast for a coast-attached dam) and gradually decreases towards the seaward end(s) of the dike, until it quickly goes to zero very close to the dike tip. The hydrostatic force on the dike associated with this head difference, integrated over the full dike length, will once more yield the net resulting tidal force on the DTP dike as given by Eqation (1). Based on this theory, Hulsbergen (2005) introduces a rather simple and straightforward expression for the maximum head difference amplitude over a straight DTP dike:

$$\Delta h_{max} = 2\omega V_{max} L/g \qquad (3)$$

in which:

Δh_{max} Maximum head difference amplitude (half-way along the dike or at the coast);

ω Angular tidal frequency of the tidal signal ($\omega = 2\pi/T$);

V_{max} Undisturbed tidal velocity amplitude;

L Representative length scale of the dike;

g Gravitational acceleration (9.81 m/s^2).

In his analysis of coastal DTP dikes with Coriolis-induced Kelvin wave, Mei (2012, 2020) takes a different mathematical route but ultimately arrives at this same Equation (3) for cases in which diffraction plays only a minor role (dam length $L \ll$ tidal wave length λ). Seen in the direction of the tidal wave, water levels on both sides of the dike will experience a phase difference $\Delta\phi$; the tide at the "downstream" side will lag some time behind the "upstream" side. For cases where diffraction and drag are unimportant, this phase lag is found to be proportional to dam length L and tidal wave number k_0 (this study): $\Delta\phi = 2k_0 L = 4\pi L/\lambda$, if $L/\lambda \ll 1$ and $V_{max} \ll 1$.

With respect to maximum head difference, here we restrict ourselves to the mathematical explanation given above. Based on the results described in this section, we now compare the head difference Δh_{max} predicted by theory to results of numerical simulations by the FINEL model, for a range of basic DTP dike types, dike lengths and tidal wave amplitudes. In all simulations, we adopt a simple west-east travelling harmonic S_2 tide with a wave period T of 12.0 h and a constant water depth of 30 m; the associated constant tidal wave length λ is equal to 741.1 km. Both bottom friction and Coriolis force are set to zero in all cases. Furthermore, as confirmed by Dai et al. (2018), model results are not sensitive to the horizontal eddy viscosity ν_H in these computations, at the given model scale and mesh resolution; hence the eddy viscosity may be either set to zero or to its molecular value $\nu_H = \nu_{mol} = 10^{-6}$ m^2/s. For the 2,000 x 1,000 km^2 sea domain a flexible triangular mesh of approximately 57,000 elements is applied, in which the resolution varies from 1 km in the direct vicinity of the DTP dam to 5 km in the far-field region near the tidal boundaries. For tidal simulation of the given type a time step of 300 sec = 5 min turned out to be suitable and the entire simulation length has been 10 days (= 20 S_2 tidal cycles). A total number of 560 FINEL runs have been made on behalf of this analysis, varying tidal ranges and DTP dike shapes/lengths.

Four different tidal ranges have been examined, leading to corresponding tidal (flow) amplitudes:

Tidal range **$(2a)$**	**Tidal amplitude** **(a)**	**Tidal velocity amplitude** **$(V_{max} = a\sqrt{g/D})$**
0.002 m	0.001 m	0.0005718 m/s
0.02 m	0.01 m	0.005718 m/s
0.2 m	0.1 m	0.05718 m/s
2.0 m	1.0 m	0.5718 m/s

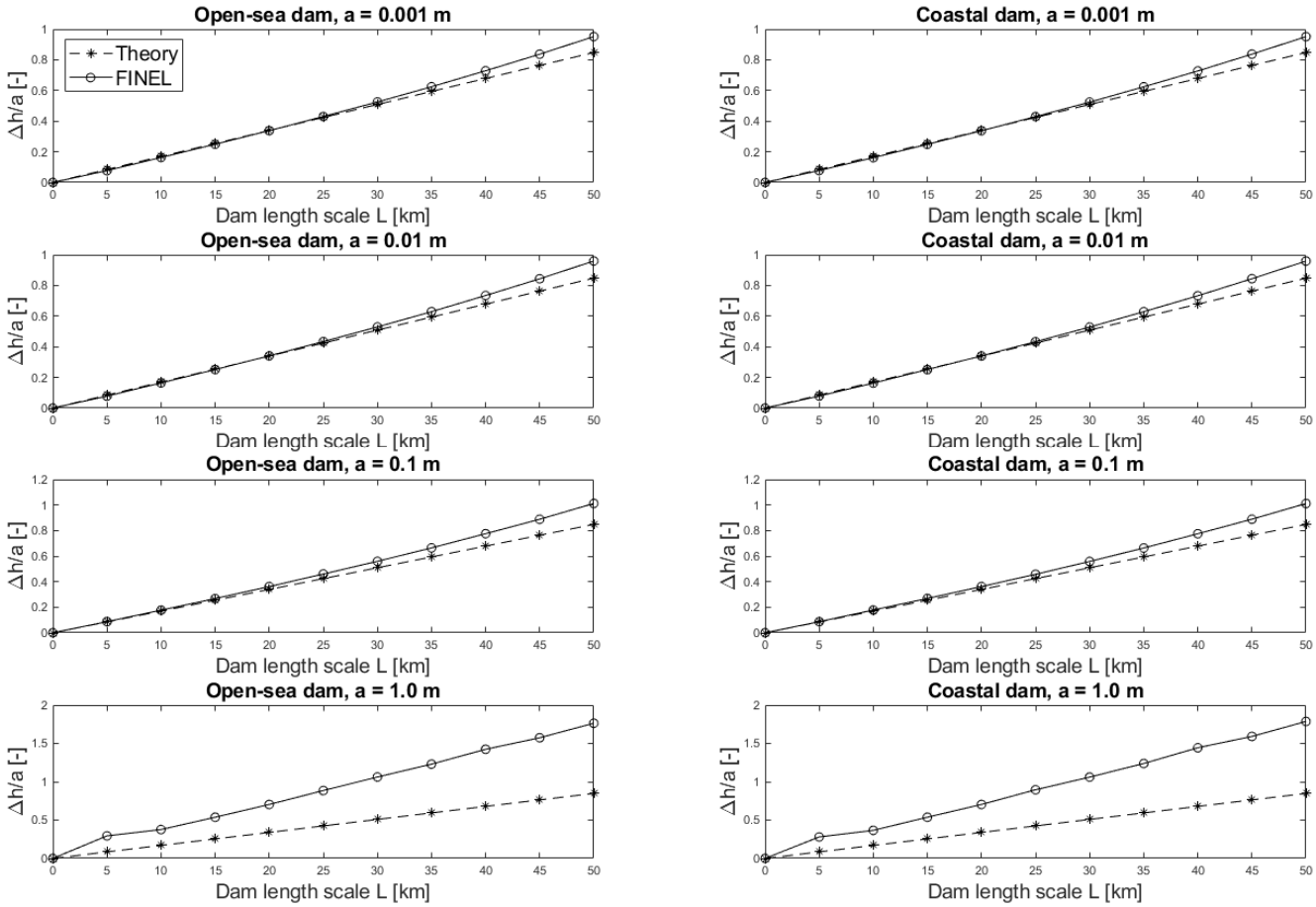

Figure 2: Head difference $\Delta h_{max}/a$ (normalized by tidal amplitude) for open-sea dams (left panels) and coastal dams (right panels), for tidal amplitudes of 0.001 m, 0.01 m, 0.1 m and 1.0 m (FINEL versus theory).

In Figure 2, we compare the values of Δh_{max} as computed by FINEL with the theory of Equation (3), for open-sea DTP dams (left) and coastal dams (right), for four difference tidal amplitudes. (We consider the straight DTP dike from Figure 1, without any extensions.) It can be observed that FINEL results and (linear) theory match well for relatively small tidal amplitudes and not too long DTP dikes. For amplitudes up to $a = 0.1$ m and (half) dam lengths up to $L = 25$ km, the match is almost perfect. For $L > 25$ km in the present case, we observe that larger-scale wave diffraction effects start to play a role and theory will give an underprediction of Δh_{max} relative to the numerical model; approximately starting from (half) a dam length L > 5-10% of the tidal wave length, such diffraction effects appear to become important. The scattered diffraction wave is also called a "parasitic wave" (Dai et al., 2018). The present situation seems favourable in terms of diffraction, because FINEL predicts a larger Δh_{max} (and hence a larger energy harvest) than linear theory. However, this advantage may not always be there; on the contrary, for instance, for truly very long DTP dikes (e.g. more than 100's of km's length), the diffracting wave may simply have insufficient time during a tidal period to fully reach and exploit the maximum head difference.

For a tidal amplitude of $a = 1.0$ m (lower panels), we observe a large deviation between theory and numerical model: compared to Equation (3), FINEL predicts a Δh_{max} that is almost twice as high. A closer look on the tidal signal in this case, however, reveals that tidal non-linearity is quite important in this case. In accordance with observations made by Dai et al. (2018), we observe that the tidal wave severely distorts over time and space and grows increasingly asymmetric due to non-linear convection. Moreover, because tidal asymmetry evolves with wave travelling distance,

the resulting Δh_{max} is strongly location-dependent (!). In this case, the peak acceleration dV/dt in Equation (1) cannot be approximated anymore by ωV_{max} in Equation (3), but must be replaced by the undisturbed non-linear peak acceleration $(dV/dt)_{max}$ instead. If we apply this correction to Equation (3), the difference between FINEL and theory in the lowest two panels of Figure 2 is already reduced by 70%. It is very likely that the remaining 30% can be accounted for by the drag term, because it is observed from FINEL results that drag forces are important for $a = 1.0$ m (alternating flow separation regions behind the DTP dam are actually observed!), which is not surprising due to the relatively large KC number (of order 1 and larger) which indicates that drag forces are not negligible anymore.

We now turn to a series of adapted DTP dikes, in which a simple watertight straight dike is supplemented with one or more perpendicular "bars" on its end points (without turbines). This can be done in order to avoid energy loss due to "leakage" around the dam tip and also to distribute the head difference Δh_{max} more equally over the dam length (uniformly instead of elliptically).

In Figures 3 and 5 we show various types of "L-shaped" dams, in which bars are either oriented westward or eastward; furthermore, these types can be combined into a so-called "T-shaped" dam (Figure 7), both for open-sea dikes and dikes attached to the coast. One may obviously ask the question whether Equation (3) is also able, in any adapted form, to predict the maximum head difference for these L-shaped and T-shaped dams. This is indeed possible, in a surprisingly simple way: in Figures 3, 5 and 7, it is easy to make the interpretation that the L- and T-shaped bars actually *increase the added mass region* (shown in gray), so that it becomes virtually oval instead of circular. If the increased added mass volume m_a is computed and substituted into Equation (1), a straightforward extension to Equation (3) is found:

$$\Delta h_{max} = (2L + (4/\pi)B)\omega V_{max}/g \qquad \text{for L-shaped dams (left and right)} \qquad (4)$$

$$\Delta h_{max} = (2L + (8/\pi)B)\omega V_{max}/g \qquad \text{for T-shaped dams} \qquad (5)$$

in which:

L Length scale of the turbine-containing dike segment;

B Length scale of the L- or T-shaped perpendicular bars.

In Figures 4 and 6, we compare this extended added-mass theory to corresponding FINEL results, for left-oriented and right-oriented L-shaped dams, respectively; in Figure 8, we do the same for a series of T-shaped dams. In all cases we use $L = 25$ km (or equivalently $2L = 50$ km) for the turbine-containing dike segment; the length B of the bars is varied between 0 and 50 km. We consider only two different amplitudes ($a = 0.001$ m and $a = 1.0$ m) and in all Figures 4, 6 and 8, we have plotted the results for open-sea dams and coastal dams simultaneously, as these results do actually almost perfectly coincide. For $a = 0.001$ m and a bar length $B < 15$ km, it can be observed that FINEL results and the extended theory from Equations (4)-(5) are in agreement. For longer L-shaped or T-shaped bars, diffraction becomes once more important; and moreover, in between the bars a significant reflection effect will occur for larger values of B. One can even argue (and this has been confirmed by some FINEL experiments) that a significant wave amplification (resonance!) will occur if B approaches one quarter of the tidal wave length. This however would imply a B value of 100's of km's, hence this case will be entirely unimportant in practice. Finally, it is noteworthy that the orientation of the L-shaped bars (left of right) actually has hardly any influence in terms of the resulting head difference (!).

For a tidal amplitude of $a = 1.0$ m, again we observe a large deviation between theory and model results, which once more is caused by the strong tidal non-linearity (due to convection, see Dai et al., 2018) and the importance of drag for relatively large KC number. This is true for both the L-shaped and T-shaped dams. Again, if the factor ωV_{max} in Equation (4)-(5) is replaced by the non-linear peak acceleration $(dV/dt)_{max}$, the error may be reduced by 70-80% already; probably the remaining error is largely accounted for by drag forces.

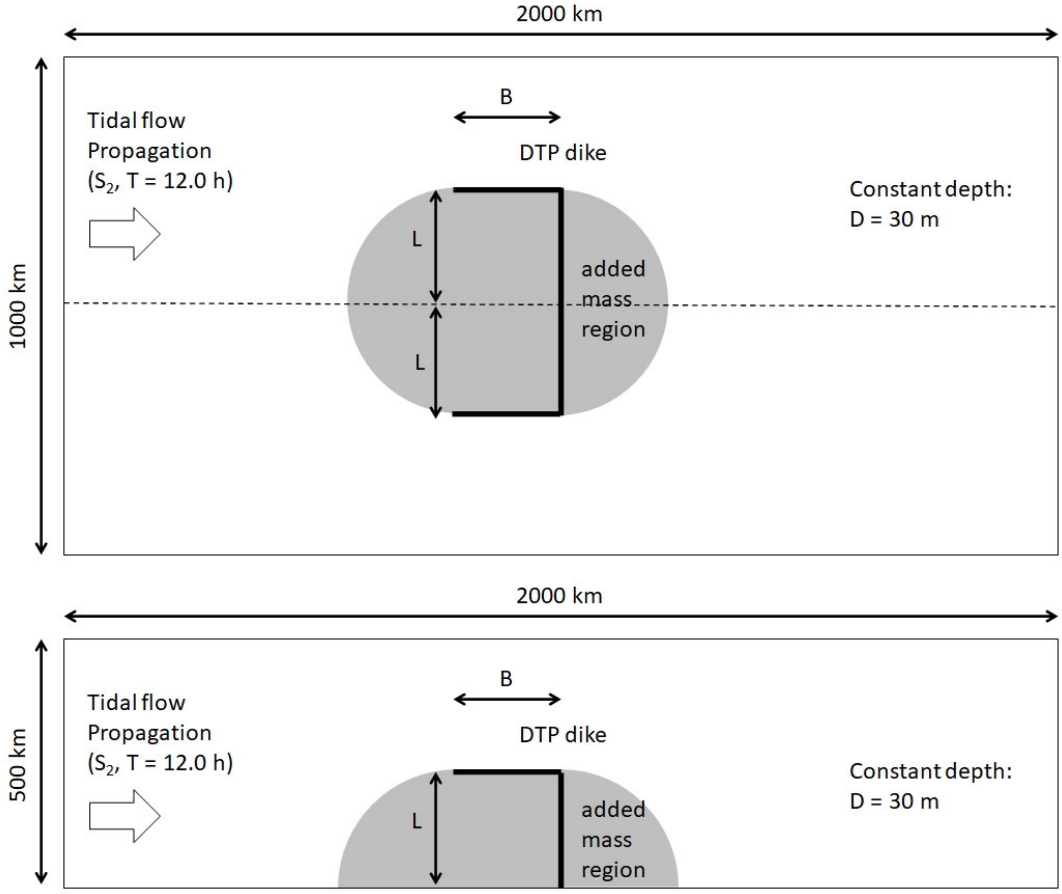

Figure 3: Lay-out of a DTP dike with left L-shaped bar, with the circular "added mass" region around the DTP dike indicated in light gray. Upper panel: detached open-sea DTP dike, lower panel: coast-attached DTP dike.

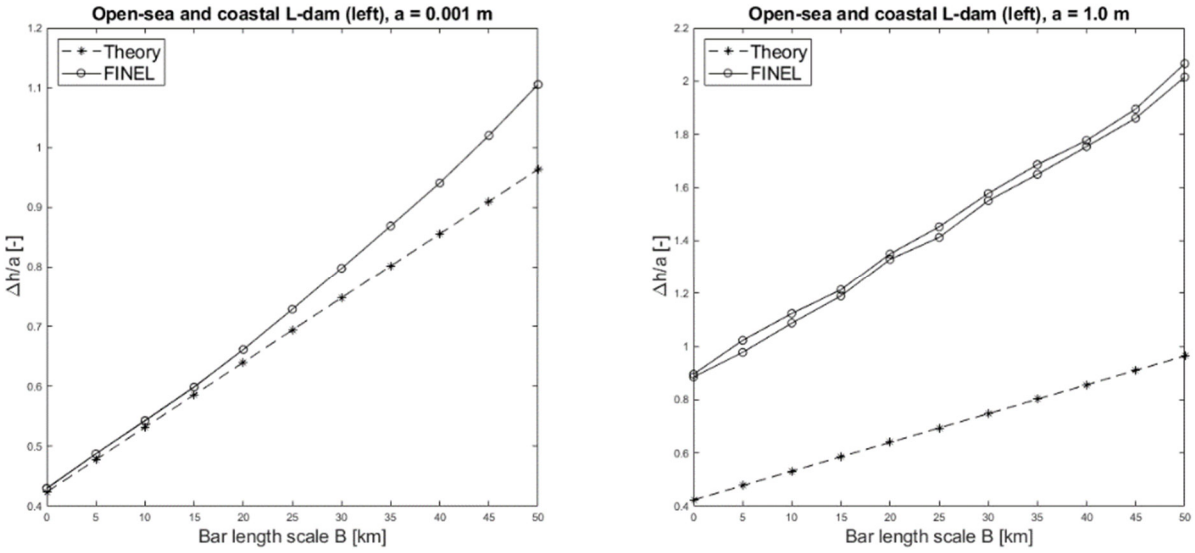

Figure 4: Head difference $\Delta h_{max}/a$ (normalized by tidal amplitude) for open-sea dams and coastal dams simultaneously (left-oriented L-dams), for tidal amplitudes of 0.001 m and 1.0 m (FINEL versus theory).

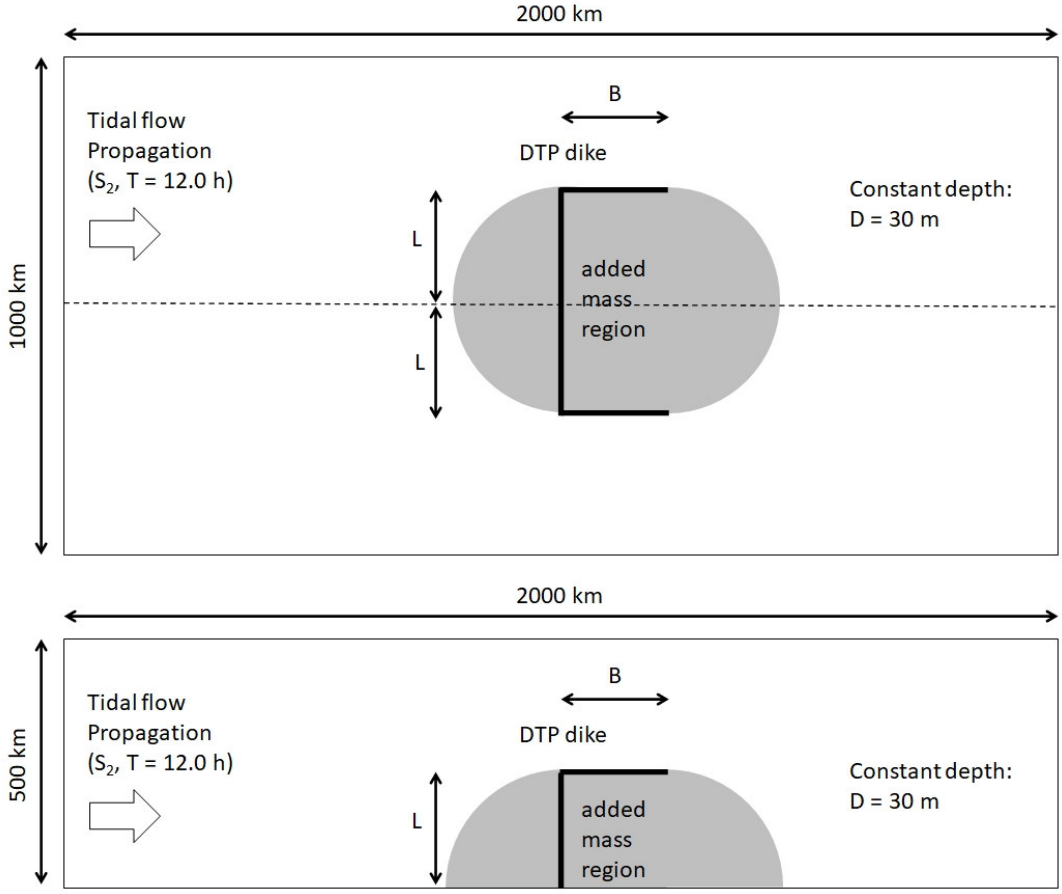

Figure 5: Lay-out of a DTP dike with right L-shaped bar, with the circular "added mass" region around the DTP dike indicated in light gray. Upper panel: detached open-sea DTP dike, lower panel: coast-attached DTP dike.

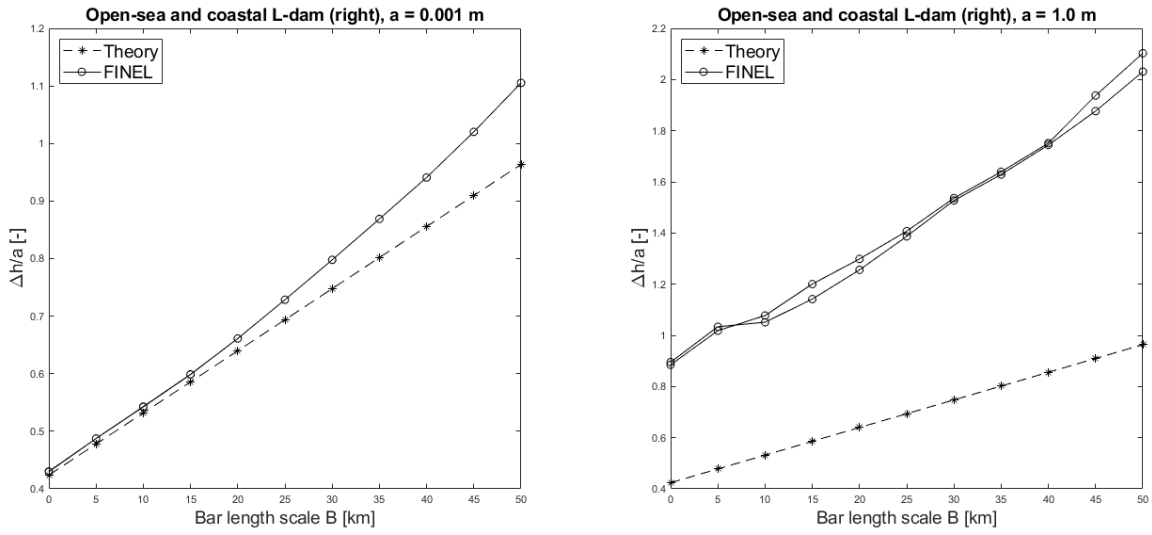

Figure 6: Head difference $\Delta h_{max}/a$ (normalized by tidal amplitude) for open-sea dams and coastal dams simultaneously (right-oriented L-dams), for tidal amplitudes of 0.001 m and 1.0 m (FINEL versus theory).

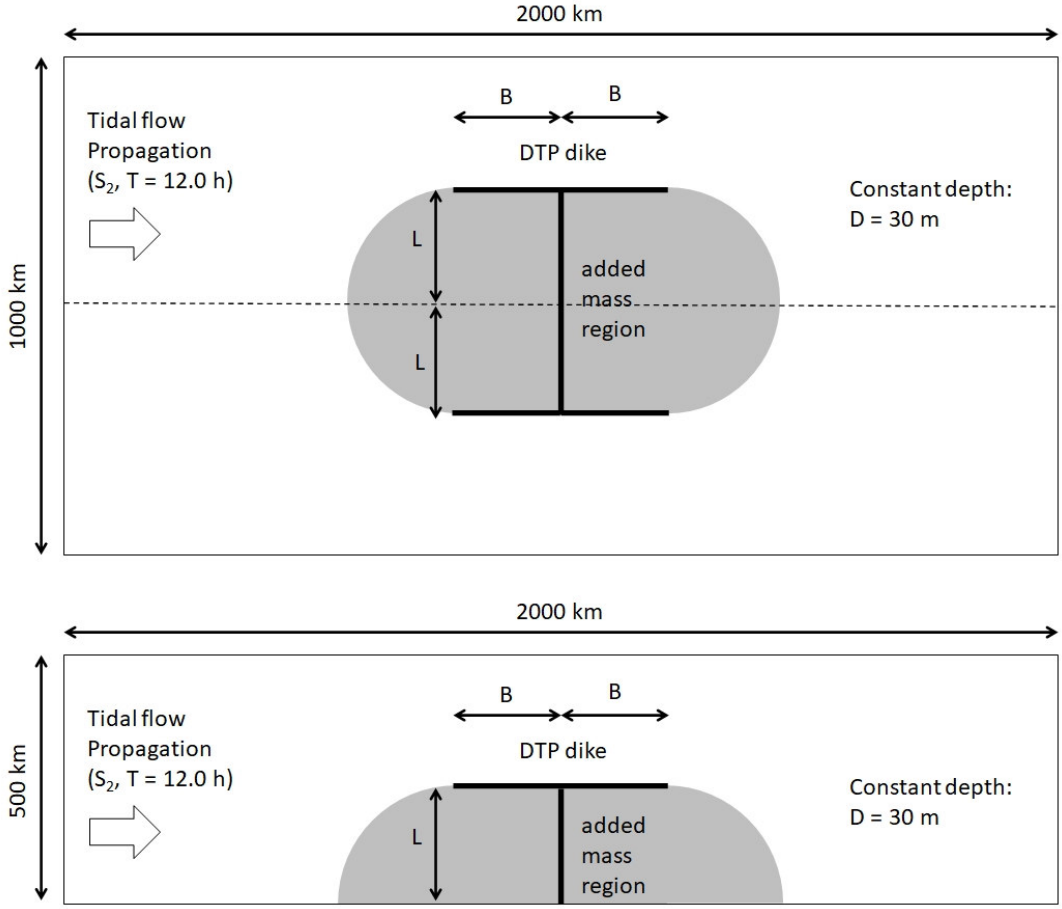

Figure 7: Lay-out of a DTP dike with T-shaped bars, with the circular "added mass" region around the DTP dike indicated in light gray. Upper panel: detached open-sea DTP dike, lower panel: coast-attached DTP dike.

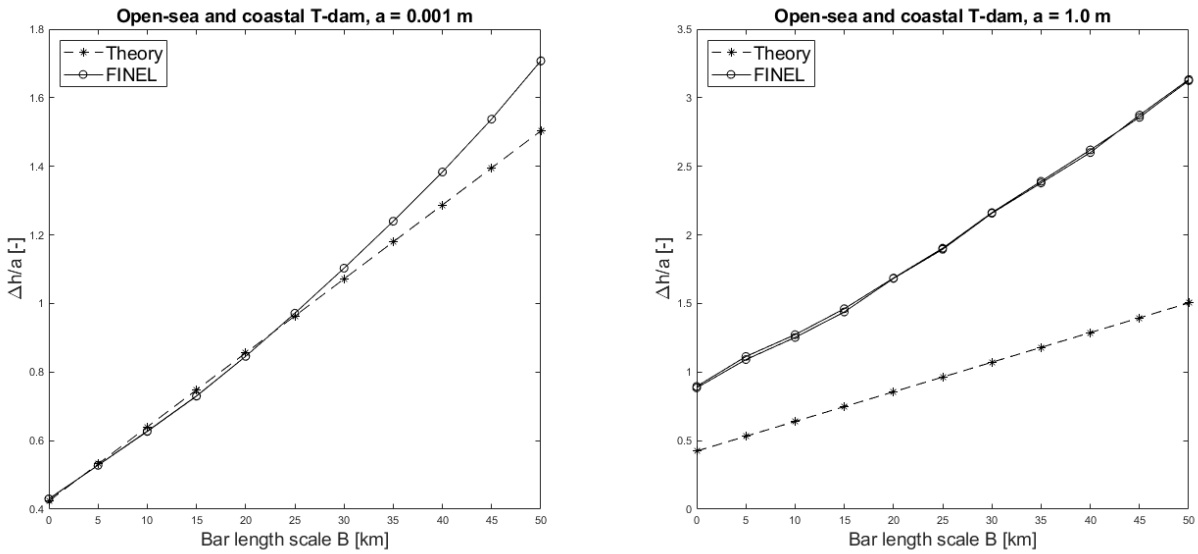

Figure 8: Head difference $\Delta h_{max}/a$ (normalized by tidal amplitude) for open-sea dams and coastal dams simultaneously (T-dams), for tidal amplitudes of 0.001 m and 1.0 m (FINEL versus theory).

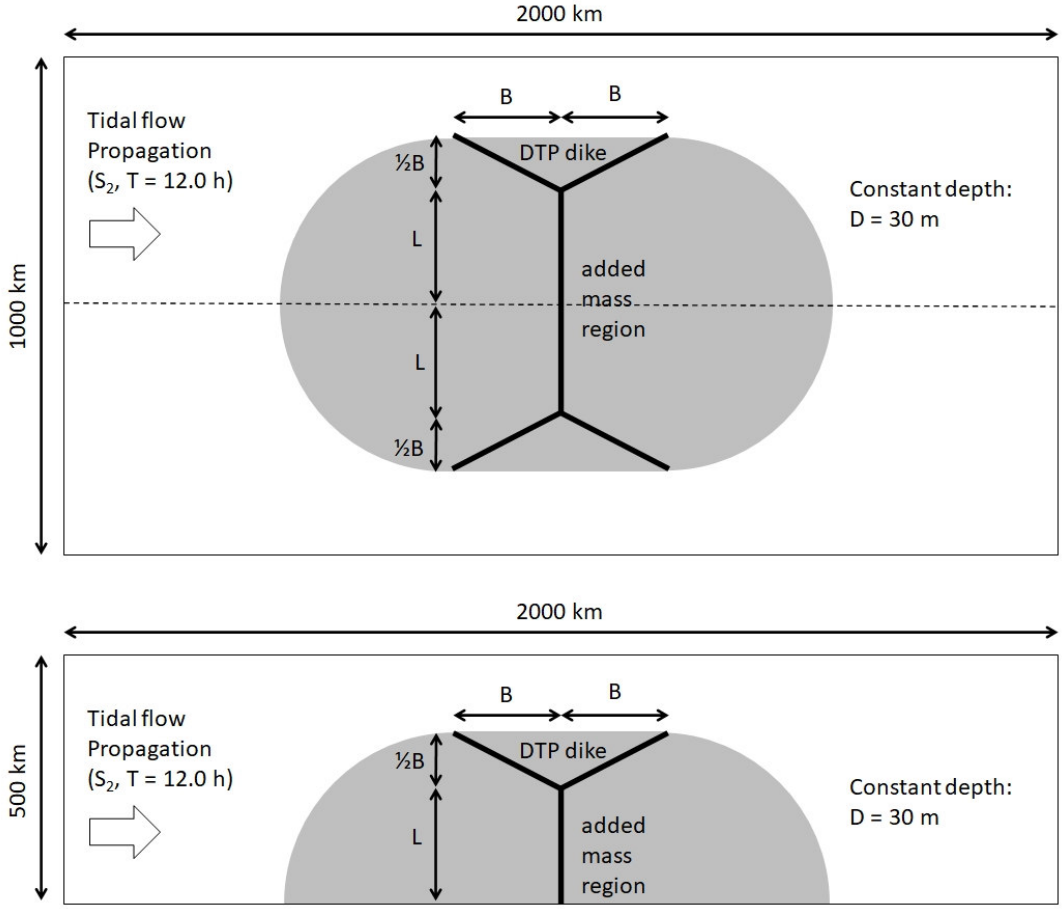

Figure 9: Lay-out of a DTP dike with Y-shaped bars, with the circular "added mass" region around the DTP dike indicated in light gray. Upper panel: detached open-sea DTP dike, lower panel: coast-attached DTP dike. (In this specific case, the "slope" of the Y-shaped bars is chosen to be ± 0.5.)

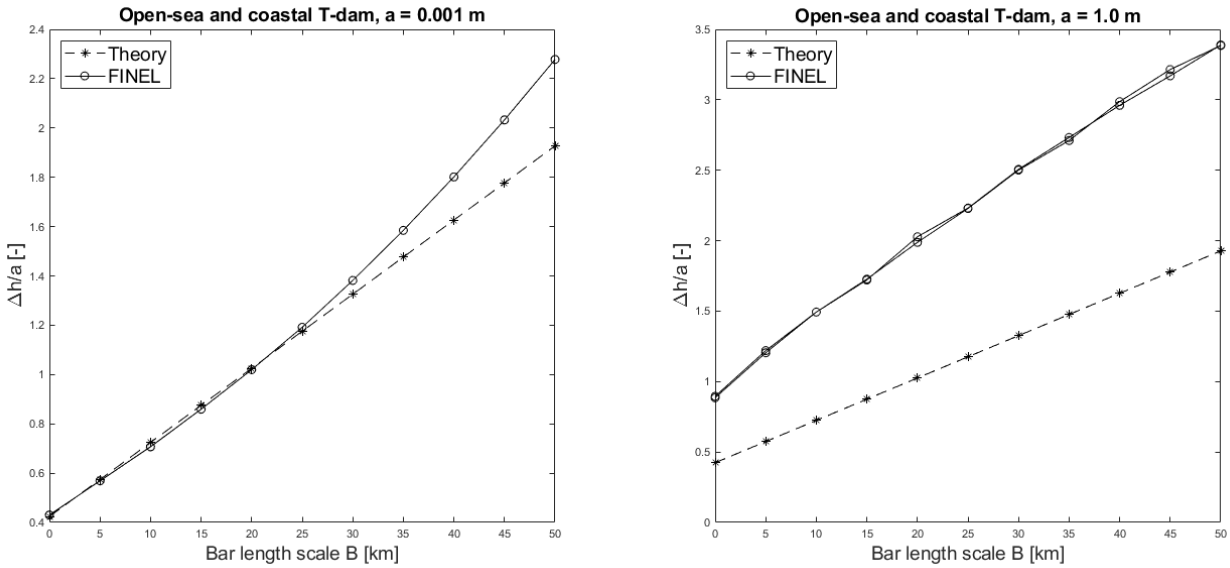

Figure 10: Head difference $\Delta h_{max}/a$ (normalized by tidal amplitude) for open-sea dams and coastal dams simultaneously (Y-dams), for tidal amplitudes of 0.001 m and 1.0 m (FINEL versus theory).

Finally, a similar analysis can be made for the case of Y-shaped dams: if the perpendicular L- of T-shaped bars are "tilted" slightly away from the turbine-containing dam segment, a Y-shaped bar will result. Based on numerical simulations by Hulsbergen (2005, 2008) and other authors, it is anticipated that Y-shaped dams actually yield the greatest values of head difference Δh_{max} among all the DTP dike types examined so far (and hence potentially the greatest energy harvest). This can be easily understood by looking at Figure 9, and observing that a Y-shaped dam actually enlarges the added-mass region in two dimensions: not only in "streamwise" direction (i.e. parallel to the undisturbed tidal flow), but also perpendicular to it (!). Therefore, it is again worthwhile to define an enlarged added mass region: this has been elaborated here for the case of Y-shaped dams with a horizontal "tilt" or slope of 0.5, i.e. a slope ratio of ½B over B (corresponding to an angle ≈ 26.5°, see Figure 9). In this case, the basic equation for Δh_{max} becomes:

$$\Delta h_{max} = (2(L + ½B) + (8/\pi)B)\omega V_{max}/g \qquad \text{for Y-shaped dams} \qquad (6)$$

In Figure 10, we compare this extended added-mass theory to corresponding FINEL results, for this specific Y-shaped dam configuration. In all cases we use $L = 25$ km (or equivalently $2L = 50$ km) for the turbine-containing dike segment; the "projected" length B of the bars is varied between 0 and 50 km. We consider only two different amplitudes ($a = 0.001$ m and $a = 1.0$ m) and again, we have plotted the results for open-sea dams and coastal dams simultaneously, as these results do very well coincide. For $a = 0.001$ m and a bar length $B < 25$ km, it can be observed that FINEL results and the extended theory from Equation (6) are in agreement. For longer Y-shaped bars, diffraction becomes once more important. For a tidal amplitude of $a = 1.0$ m, again we observe a large deviation between theory and model results, which once more is caused by the strong tidal non-linearity. Again, if the factor ωV_{max} in Equation (4)-(5) is replaced by the non-linear peak acceleration $(dV/dt)_{max}$, the error may be reduced by 70-80% already.

A sensitivity analysis for the maximum head difference amplitude and phase shift for Y-shaped dams has been performed by Liu and Zhang (2014). They confirm that Y-shaped dams are more advantageous than T-shaped dams with respect to head difference amplitude, because more of the tidal flow is being "caught" (added mass) and the narrowing of the tidal basin toward the dam makes (partial) resonance of the water body nearby the dam more likely. Furthermore, they observe that the phase difference between both sides of the Y-shaped dam could actually approach the "optimal" value of 180° under the right circumstances, provided the Y-shaped bars are sufficiently long and optimally directed: Liu and Zhang (2014) find an optimal angle ≈ 40°.

To summarize and discuss the results shown in this section:

- The basic Equation (3) for the maximum head difference over a DTP dike, as derived by Hulsbergen (2005, 2008) and Bitter (2018), is obviously valid and correct for the case of relatively small tidal wave amplitudes and dike lengths that are small compared to the tidal wave length; in this case, tidal non-linearity and drag as well as wave diffraction are negligible.
- However, it can also be observed that, for "realistic" tidal amplitudes (order of 1-2 m) and realistic DTP dike lengths (of order 50 km), both tidal asymmetry and wave diffraction become important already. Moreover, the applicabiliy range of Equation (3) is unfortunately *limited on two sides*: the DTP dike may not be too short (in order to exclude drag forces) neither too long (in order to exclude diffraction). Physically, hence, we are bound to navigate carefully in between two unwanted extremes.
- This means that, even in the present idealized case without topography or bathymetry, the linear theory of the present section yields only indicatory results at best. Furthermore in real-life applications tidal asymmetry will always be present, not to speak about the presence of a wide range of tidal wave components which form a spectrum together. The

use of a numerical model for both theoretical and practical purposes therefore remains vital for any DTP design process (!).

- As recalled by both Hulsbergen (2005, 2008) and Bitter (2018), a series of explorative numerical DTP simulations near the IJmuiden harbour region resulted in a large difference between linear theory and numerical results (by the Rijkswaterstaat ZUNOWAK model), of about a factor 1.7 (i.e. a deviation of 70%). It has been noted by both authors that this factor 1.7 contains many site-specific influences, such as bathymetry, drag, Coriolis force (Kelvin wave) and bottom friction. In addition to this list, we note here that even the amphidromic point in the Soutern North Sea may shift westward (!) due to the presence of a DTP dam along the Dutch coast, which may in turn enhance the longshore tidal range. However, the present study clearly shows the great importance of tidal non-linearity for real-life tidal amplitudes; the figures in this section show that even stand-alone tidal asymmetry is already able to easily account for the factor 1.7 deviation found near IJmuiden. This underlines the importance of numerical models that contain all non-linear, topographical and geophysical phenomena.
- A more principal point is that the above linear DTP theory strongly relies on undisturbed tidal velocity, whereas there is no such thing like an "undisturbed" velocity if the tide is actually disturbed by an obstacle, especially in case of non-uniform topography. Only by grace of the assumption of negligible diffraction (for short DTP dikes) this issue can be circumvented, at least for theoretical cases.
- It is however good news that the impact of L-shaped, T-shaped and Y-shaped bars attached to the main DTP dike can be so easily estimated in a global way, by extending the added-mass theory within Morison's Equation (1) for bars of various shapes and types. This supports the idea that added mass combined with the peak tidal acceleration (i.e. tidal flow inertia), plays a central physical role indeed.
- From the figures in this section it can be concluded that the cases of coast-attached dikes and detached open-sea dikes are fully equivalent, both in results and in KC number range, if the open-sea dam case is viewed as being a coastal dam case which has been actually mirrored across the coastline. To this end, the KC number must be based upon *half* the DTP dike length for open-sea dams and on the *full* dike length for coastal dams.
- The above conclusions indicate that the physical principe behind DTP does "work" indeed. Of course, however, this has only been proven by means of numerical modelling, not only by the present study but also by previous authors. The reason for this, obviously, is that a true field experiment for DTP dams would be tremendously costly on prototype scale. It is therefore worthwhile to consider whether (and how) the basic principle of Dynamic Tidal power could be tested on laboratory scale, yet in such a way that the results are still sensible and applicable for prototype purposes. This is a key challenge for the near future.

4 INFLUENCE OF THE EARTH'S ROTATION AND TIDAL DIFFRACTION

The DTP hydrodynamic theory discussed so far has been based on the rather macroscopic concepts of "added mass" and ambient undisturbed tidal acceleration, decribed by a Morison-type equation. This has lead to basic Equation (3): a straightforward expression for the maximum head difference amplitude over a straight DTP dike (Hulsbergen, 2005). In the present section, we briefly describe the extended analysis by C.C. Mei (2012, 2019, 2020), who incorporates the influence of the Earth's rotation (Coriolis force) and tidal diffraction into the theory of DTP hydrodynamics.

Earlier work on tidal diffraction problems along a coastline has been performed by Buchwald (1971, 1974). Based upon Buchwald's analytical functions, Mei (2012) solves the problem of diffraction analytically by a straight (watertight) DTP barrier perpendicular to a straight coast. Once more, the geometry is idealized to constant sea depth, a thin and vertical barrier and a monochromatic harmonic tidal signal. The influence of Coriolis force is however included. By this

analysis two different types of Coriolis-driven waves are distinguished, which are scattered by the barrier. First a Kelvin wave is present, which balances the earth's Coriolis force against a topographic boundary such as a coastline. Second, for tidal frequencies greater than the Coriolis frequency also a Poincaré wave may be present, which can be seen as an internal rotation-driven two-dimensional oscillation of the tidal wave. The latter (dispersive) wave can also be present at open sea, whereas the former (non-dispersive) wave needs the presence of a (coastal) boundary in order to exist. The presence of Kelvin waves can make DTP dikes attached to a coastline especially attractive, as the maximum tidal range in coastal seas is often found near-shore.

In his very elaborate analytical calculations, Mei (2012) uses the method of "matched asymptotics" to derive the scattered wave field around a coastal DTP dike, which is valid for cases in which the dike is much shorter than the tidal wavelength, $L \ll \lambda$ (!). In Mei (2020), this analysis is extended toward the theoretical case of tidal diffraction by a small island or cape of (semi-)elliptical shape. Ultimately, at least for the case in which $L \ll \lambda$, Mei (2012, 2020) arrives at precisely the same expression as Hulsbergen (2005) for the head difference amplitude over a relatively *short* DTP dike, namely Equation (3). Moreover, Mei (2012) proves that the spatial shape of the head difference amplitude is indeed elliptic, which leads to a more complete equation (for dikes without bars):

$$\Delta h(x) = 2\omega V_{max}\sqrt{L^2 - x^2}/g \qquad (7)$$

in which:

$\Delta h(x)$ Head difference amplitude along the dike;

ω Angular tidal frequency of the tidal signal ($\omega = 2\pi/T$);

V_{max} Undisturbed tidal velocity amplitude;

L Representative length scale of the dike;

g Gravitational acceleration (9.81 m/s^2);

x Longitudinal coordinate along the dike (varying as $0 < x < L$ for attached coastal dikes and $-L < x < L$ for detached open-sea dikes). Equation (7) reduces to (3) for $x = 0$.

It is encouraging that both an asymptotic diffraction theory and macroscopic added-mass theory are actually in agreement with respect to head difference. However, this is only the case for $L \ll \lambda$; larger-scale diffraction effects which may occur for longer DTP dikes (as shown in Figures 2, 4, 6, 8 and 10) are not included in both theories and require numerical modeling to be assessed.

5 INFLUENCE OF A PARTIALLY OPENED DTP DIKE; DISCHARGE AND POWER OUTPUT

In the above analysis, all dikes discussed so far were "watertight". It is however obvious that in reality DTP dams will always be partially open dams, due to the presence of a large concentration of energy turbines. It is anticipated by various authors (Mei 2019, Bitter 2018, Hulsbergen 2008) that these turbines will have a relatively small rotation speed and a relatively large radius or diameter compared to their mutual spacing (heart-to-heart distance), in order to optimally exploit the locally present head difference in a mechanically optimal way.

Energy turbines utilize the local head difference to generate a sea water discharge and hence an energy output; on the other hand, however, they compromise the DTP dam's effectiveness by reducing the same head difference. Dependent on its mechanical design, each turbine can be characterized by a relation between discharge and head loss (Q-H curve) which will not only determine the effective head difference across the DTP dam, but also its energy efficiency. An optimal trade-off between between flow discharge and head loss needs to be sought during DTP design in order to find the best turbine concentration and hence optimal energy output. Sufficient knowledge of the design characteristics of each turbine type (in terms of Q-H curve) will be vital.

In anticipation of "true" Q-H curves coming available (belonging to the design specifications of various types of real energy turbines), it is worthwhile to make a first estimate of the relation between discharge and head difference across the DTP dam that can be expected. Mei (2019, 2020) and Bitter (2018) describe two different approaches to estimate the discharge Q and power output P based upon a pre-calculated head difference $\Delta h(x)$; in addition, Svašek Hydraulics uses another simple method to apply a given Q-H curve directly to the FINEL numerical model of a DTP dike, which also yields a correct physical coupling (feedback) between Q and Δh. (This latter approach will be applied to North Sea calculations in the remainder of this report.)

To start with the latter approach: a partially opened DTP dike can be conceptually modelled by means of a simple barrier/gate formulation, in which the DTP dike (which extends from the sea bed all the way to the water level) is opened half-way the water column, over a height H and over the full length of the dike. Through this gate, a fully submerged and sub-critical barrier flow will develop. Taking quasi-stationary flow through the gate (which implies that flow velocity adapts to local head difference instantaneously) and assuming that flow velocity upstream of the gate is small compared to the velocity inside the gate itself, the Q-H curve describing discharge through the gate reads:

$$q = C_d H \sqrt{2g(\Delta h)} \tag{8}$$

in which:

$q(x,t)$ Discharge through the dike gate, per unit width [m^2/s];

$\Delta h(x,t)$ Head difference amplitude, varying along the dike [m];

C_d Discharge coefficient [-];

H Gate height, present along the entire dike length [m].

Usually, the value of the discharge coefficient C_d will be close to 1.0, as we assume that outflow from the gate results in a maximum energy height loss (equal to the full velocity height). If the resulting specific discharge $q(x)$ is integrated over the dike length, a total discharge Q is found. We observe that a basic Q-H curve for a submerged gate or energy turbine is of the general form:

$$Q \sim \sqrt{\Delta h} \tag{9}$$

If the gate height H is divided by the water depth D, a ratio $\alpha = H/D$ can be defined which stands for the relative permeability or "leakage" of the dike. For their simulations of the case of a 40 km long straight DTP dike near IJmuiden, Hulsbergen et al. (2008) report that each % of dam opening would account for a loss of head difference of about 3.6%, which implies that a value of $\alpha = 10\%$ would lead to an effective 36% head loss. It is anticipated by Svašek and by the former authors that $\alpha = 10\%$ seems a good order of magnitude for the maximum allowable "leakage" of a DTP dike.

Mei (2019, 2020) applies a similar but slightly different approach to calculate the discharge Q and power output P. Each turbine is housed in a submerged tunnel of constant radius R. Using Toricelli's law, the discharge rate through each turbine at a given time level is given by:

$$Q = C_d \pi R^2 \sqrt{2g(\Delta h)} \tag{10}$$

The expression for local and instantaneous power output of such a turbine is of the general form:

$$P = C_e \rho g Q \Delta h = C_e C_d \rho g \pi R^2 \sqrt{2g} (\Delta h)^{3/2} \tag{11}$$

in which:

C_e General turbine efficiency coefficient [-].

If the power output P from Equation (11) is integrated over time and summed over all turbines present within the dike (using Equation (8) for the spatial variation of Δh), a total DTP power output is found as a function of time. This result can be used to find the time-averaged energy

baseload and the storage capacity needed. The turbine efficiency coefficient C_e is fully empiric at this moment and further experimental verification is definitely needed in order to assess its appropriate value. Preliminary values that have been proposed in literature vary all the way in between 0.22 and 0.80, which is a rather wide range for a coefficient that has so much influence on the over-all energy output and profitability of the energy baseload. A more full mathematical elaboration of Equation (10) and (11) can be found in Mei (2019, 2020).

In a different approach by Bitter (2018), the energy harvest from each turbine is incorporated in the Q-H curve in a more direct way. Bitter applies a Bernoulli-type energy conservation law, in which energy head loss by flow deceleration and head loss by electrical power harvest is separately accounted for. Slightly rewritten in order to match the variable nomenclature used above, we get:

$$Q = \pi R^2 \sqrt{2g(\Delta h - \Delta h_{turb})/(1 + C)} \tag{12}$$

in which:

Δh_{turb} Part of head difference loss caused by power harvest [m];

C Energy loss coefficient due to deceleration on outflow [-].

It should be emphasized that this formulation also allows turbine tunnel shapes with a non-constant diameter; in that case, the radius R has the meaning of the minimum radius of the tunnel, roughly half-way the turbine rotor. More information can be found in Bitter (2018).

The expression for local and instantaneous power output of this turbine type becomes of the form:

$$P = \rho g Q \Delta h_{turb} = \rho g \pi R^2 \sqrt{2g(\Delta h - \Delta h_{turb})/(1 + C)} \Delta h_{turb} \tag{13}$$

If we define the ratio $a = \Delta h_{turb}/\Delta h$, that ratio represents the fraction of the head loss that is actually utilized for power production. Substituting this ratio into Equation (13), we obtain:

$$P = \rho g \pi R^2 \sqrt{2g/(1 + C)} (\Delta h)^{3/2} a \sqrt{1 - a} \tag{14}$$

From this result, it follows that the optimal energy harvest will be obtained if $a = 2/3$. In fact, the coefficient $a = \Delta h_{turb}/\Delta h$ can be considered as a measure for the energy efficiency of the turbine. Whether this coefficient actually has the value $a = 2/3$ or not, will fully depend on the actual turbine design and its technical specifications.

If the power output P from Equation (14) is integrated over time and summed over all turbines present within the dike (using Equation (8) for the spatial variation of Δh), a total DTP power output is found as a function of time. This result can be used to find the time-averaged energy baseload and the storage capacity needed.

A drawback of the expressions for the energy output P as proposed by Mei (2019, 2020) and Bitter (2018) is that the applied discharge Q is not yet allowed to impose a (negative) feedback on head difference Δh, although these quantities should be dynamically coupled. In fact the expressions (10)–(14) should be coupled to a numerical model like FINEL in order to fully assess the influence of partial dike permeability on the dynamic tidal flow around the DTP dike. Bitter (2018) proposes an explicit correction factor in order to estimate the influence from Q upon Δh, which reads:

$$\Delta h_{corr} = \Delta h[1 - (Q/V_{max}S)^2] \tag{15}$$

in which:

Δh_{corr} Corrected head difference across the dike;

Δh Predicted head difference across the dike, used at first to compute discharge Q;

S The “wet surface” of the DTP dike (basically dam length times water depth).

This approximation is based on the assumption that Toricelli’s Law (see Equation (10)) remains valid even for a DTP dam that is 100% “open”; this assumption, however, is generally not correct.

Also, the problem remains that the partial opening of the DTP dike should actually affect the dynamics of the ambient tidal flow around the dike, as well as the size of the added mass region (!). Therefore, according to the authors of this memorandum, an accurate and applicable estimate of the power production of a DTP dike should always follow from the incorporation of a turbine Q-H curve into a larger numerical model, in which the head difference Δh and discharge Q are truly dynamically coupled.

Furthermore, in view of the significant differences between the Q-H curve and power output expressions as derived by Mei (2019, 2020) and Bitter (2018), it is clear that there is a great need of knowledge about design specifications of really existing energy turbines suitable for DTP, e.g. a realistic Q-H curve and an experimental verification of the various discharge coefficients and energy efficiency coefficients. This is probably one of the most crucial new steps that must be taken unto the path of further research on DTP; it would be even desirable that the experimental verification of such energy turbine specifications takes place on full prototype scale, possibly for a single turbine. Only after taking this step, and inserting the result into a larger-scale numerical model for correct dynamical coupling, it is worthwhile to make further estimations about the over-all power output of a DTP baseload.

6 PRACTICAL APPLICATION: NUMERICAL SIMULATION OF DTP IN THE NORTH SEA

To complete the picture of hydrodynamic aspects of Dynamic Tidal Power, this section illustrates the practical effects of DTP in a real marine environment.

Svašek Hydraulics (2019) has performed various numerical calculations (using FINEL) to estimate the effectiveness of DTP in the southern North Sea, applying the complete tidal signal consisting of many tidal components. The series of calculations addresses a number of DTP dike shapes and configurations on various locations along the Dutch coast; the general framework in which these configurations are modelled is the European Continental Shelf Model (ECSM). This large-scale tidal model allows us to compare the effects of single and multiple DTP dikes in a real-time situation. In principle both small-scale and large-scale effects of DTP dikes on hydrodynamics and morphology of the marine system can be examined. In this memorandum, we restrict ourselves to a limited amount of model output: the maximum head difference and maximum perpendicular flow velocity over the DTP dikes considered (which determine the over-all discharge through the turbines).

Obviously, the North Sea domain under consideration contains complexities that are not present in the idealized model cases of the previous sections:

- Tidal asymmetry and free-surface effects are omnipresent;
- In the North Sea situation a DTP dike will virtually never be of negligible length compared to tidal wave length, so that reflection and diffraction effects are important;
- The actual tide consists of many constituents and is therefore non-symmetrical and non-harmonic;
- Bottom topography and spatially variable bed friction and Coriolis force are present;
- A fully dynamic coupling between the presence of (partially open) DTP dikes and the ambient tidal flow is given by the set-up of the numerical model.

Because of these non-negligible aspects, a full numerical model will add value above simple analytical parametrizations for all cases on behalf of practical design (Hulsbergen 2008, Mei 2019).

In the FINEL-ECSM model at hand, DTP dikes/barriers can be modelled as being infinitely thin structures with infinite height. As explained in Section 5 (see Equation (8)–(9)), the partial opening of such a structure can be simulated in a conceptually simple way, using a “mailbox”-shaped gate of height H half-way the water depth and over the full length of the dike. Through this mailbox gate a fully submerged and sub-critical barrier flow will develop from one side of the barrier to the other, following the Q-H curve given in Equation (8), while FINEL applies $C_d = 1.0$ here for the

discharge coefficient needed. If gate height H is divided by water depth D, a ratio $\alpha = H/D$ can be defined which stands for the relative opening or "leakage" of the dike. In the present simulations, the vertical gap height of the mailbox gate is usually 1 meter, unless otherwise specified. This principle is illustrated in the right-hand-side panels of Figure 12.

An illustration of the FINEL finite element grid of the ECSM model is given in Figure 11. The finite element grid consists of approximately 100,000 triangular elements, which discretize water level, depth-averaged horizontal tidal flow velocity and other topographical data. The simulated period of time was January 24 to 31, 2017 (i.e. approximately 15 tidal periods).

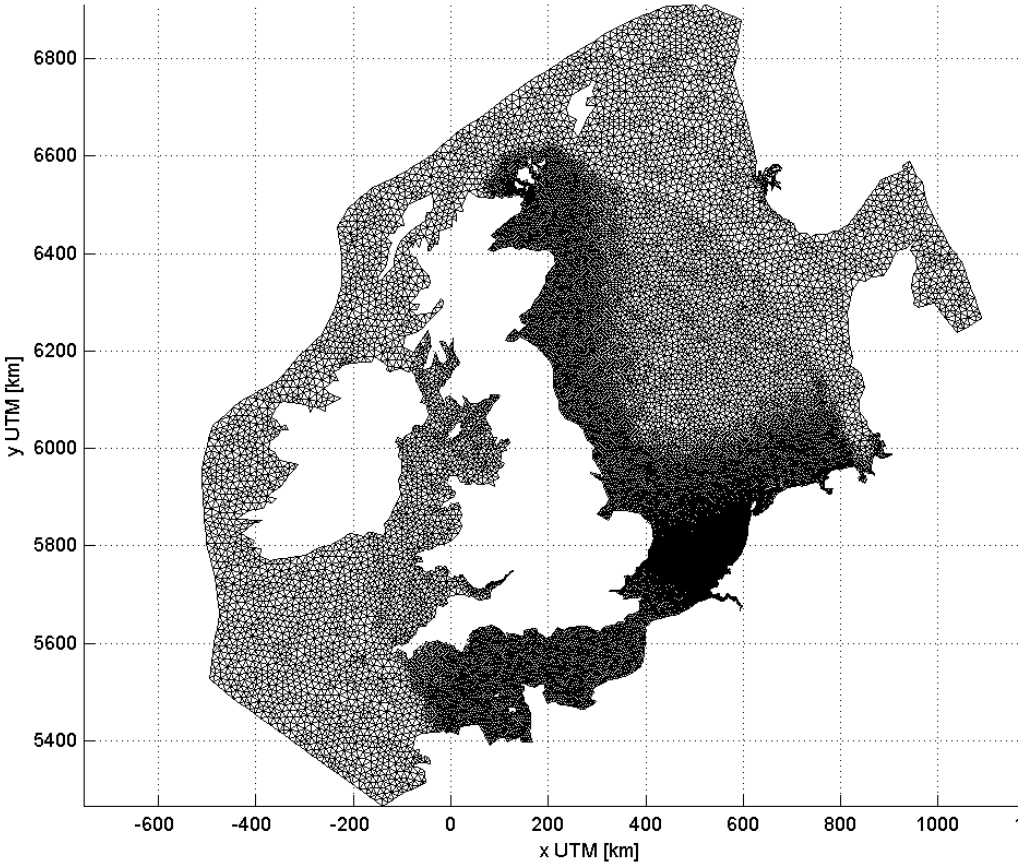

Figure 11: Outline and finite element discretization of the FINEL European Continental Shelf Model (ECSM).

Multiple barrier designs and configurations have been simulated in this study, which illustrate the way in which to find an optimal design for a DTP dike that yields the highest water head difference across the barrier. In this section, we start out with a reference case: a single open-sea DTP dike of 40 km length, just offshore of Hoek van Holland, not attached to a coast and without any L-, T- or Y-shaped bars, and roughly perpendicular to the local (long-shore) tidal flow direction, see Figure 12. Within this reference case, we vary the height of the "mailbox": this height H is being taken 0.0 m, 1.0 m and 5.0 m (see Figure 12). The reference case with H = 1.0 m has been coined "Barrier 0". Figure 13 shows the maximum flow velocity perpendicular to the DTP barrier (upper panel) and maximum head difference across the barrier (lower panel) as a function of time, for these 3 cases.

In all velocity plots the maximum local (dam-perpendicular) flow velocity for the undisturbed case without any barrier (present situation) has been added as well, in order to illustrate the impact of a watertight or partially permeable DTP dam. (This undisturbed case has been omitted within the water head plots however, because the head difference in the present situation is obviously zero.)

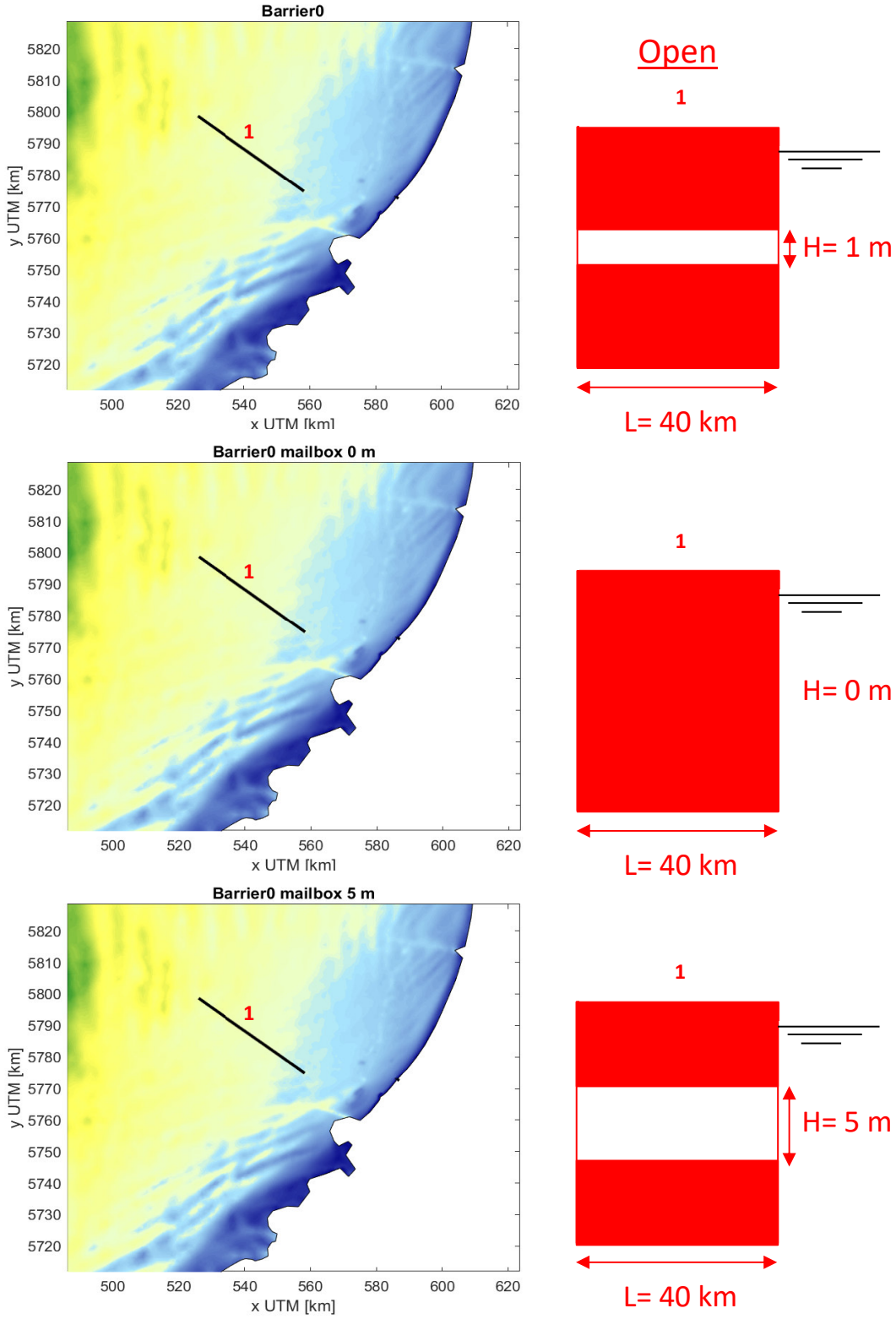

Figure 12: Reference DTP barrier configuration near Hoek van Holland (L = 40 km), with variable gate height.

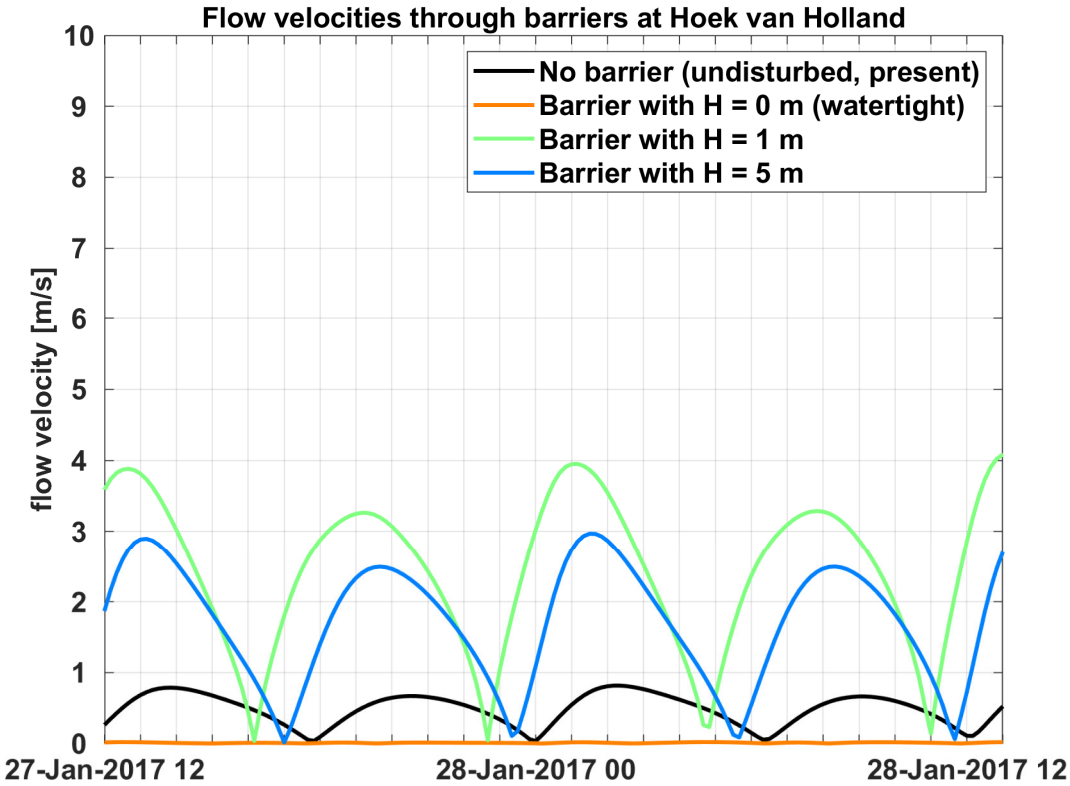

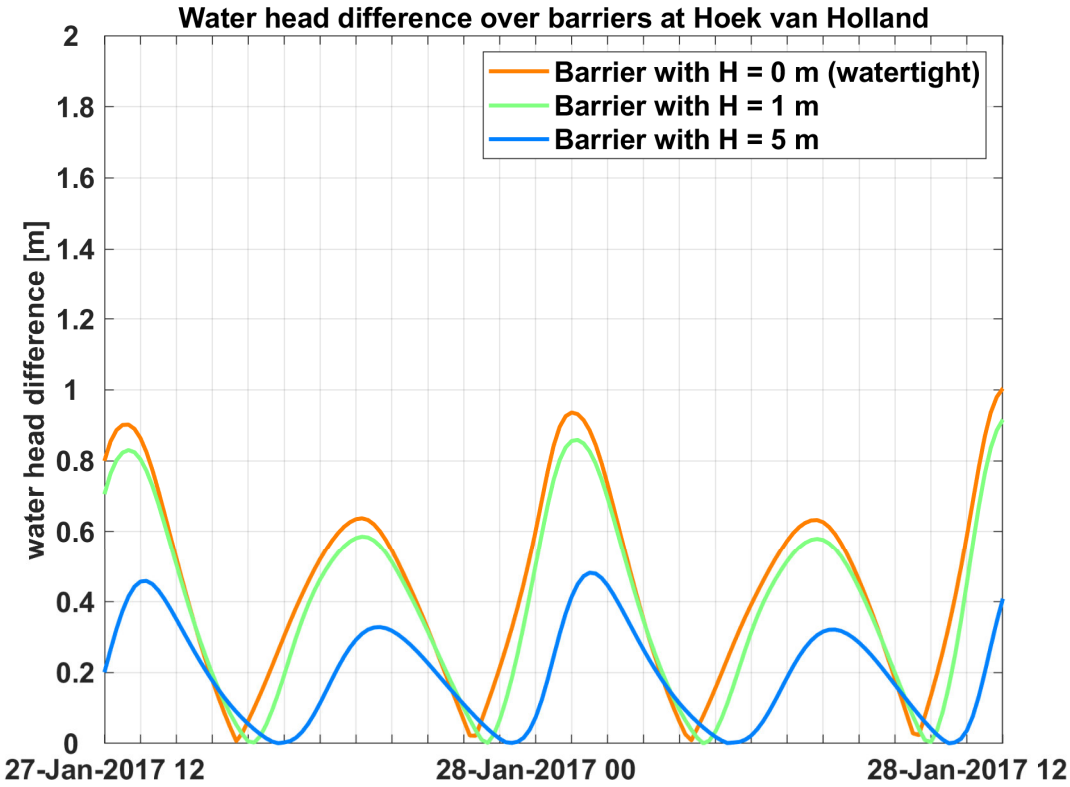

Figure 13: Maximum flow velocity perpendicular to DTP barrier (upper panel) and maximum head difference across the barrier (lower panel) as a function of time, for reference case Barrier 0 (L = 40 km) with variable "mailbox" gate height.

From Figure 13 a number of conclusions can be drawn. First of all, the greatest maximum head difference can (of course!) be found for the watertight case H = 0.0 m (the corresponding flow velocity being uniformly zero). It is worthwhile to compare this head difference with the comparable schematized DTP case which was shown before in Figures 1 and 2. It can be observed that the peak "undisturbed" local flow velocity V_{max} is of the order 0.8 m/s in the present case. Substituting this value into Equations (2) and (3), adopting a monochromatic M_2 tide and setting L to half of the open-sea dike length (L = 20 km), we find KC = 1.78 and Δh_{max} = 0.46 m. We note that for the found Keulegan-Carpenter number (> 1) the drag force becomes actually important, which is actually confirmed by flow visualisations in which flow separation and eddies can be seen. Furthermore, we observe that the maximum Δh_{max} values found in Figure 13 are actually a factor 1.5–2.0 larger than the theoretical value from Equation (3). In accordance with Figure 2, we observe that tidal asymmetry plays an important role at the given tidal amplitude, a fact that can easily account for the factor 1.5–2.0 that has been found. Also, this factor is (not surprisingly!) close to the correction factor of 1.7 which has been found earlier by Hulsbergen (2008) for the IJmuiden DTP case.

For the partially opened barrier cases (H = 1.0 m and 5.0 m), considerable perpendicular flow velocities are found which are typically several meters per second. (These perpendicular velocities U have actually been defined as $U = q/H$, in which q is the depth-averaged discharge throughout the gate per unit width.) For the reference case Barrier 0 with H = 1.0 m, the head difference only slightly decreases (less than 10%) whereas it almost decreases by 50% for the case H = 5.0 m. From flow visualizations it follows that in the latter case the over-all tidal flow mainly passes the barrier along straight streamlines (!) perpendicular to the barrier, whereas in the H = 1.0 m the flow obviously makes a much stronger "detour" around the dike, accompanied by flow separation and drag. Finally, we note that the decrease in head difference also comes with a decreasing tidal phase shift compared to the undisturbed case. These results underline that a DTP dike that is too "open" compromises its basic principle of creating an enhanced Δh_{max} by partially blocking the tidal flow. However, it should be kept in mind that the actual power output is not solely determined by Δh_{max}, but by the *product* of Δh_{max} and q (or Q) integrated along the dike length; see Equations (11) and (13). (More knowledge about realistic Q-H curves and power specifcations of designed energy turbines is vital with respect to this topic.)

Adopting the standard gate height H = 1.0 m henceforth, we will now address the influence of adding L-, T- or Y-shaped bars to the reference 40 km long dike discussed so far. Figure 14 depicts all the different alternatives that have been considered, very much in accordance with the schematized design alternatives addressed before in the Figures 1–10. As shown in Figure 14, all possible bar extensions to the main DTP dike have equal length of 10 km and are fully watertight (H = 0.0 m).

In accordance with Figures 1–10, Figure 15 shows that both the maximum head difference and maximum velocity through the barrier (and hence the maximum discharge) increase for each subsequent alternative that is considered. Because of the great influence of tidal asymmetry in the North Sea situation, no attempt is made here to "fit" the found results exactly into the framework of the Equations (4), (5) and (6). Nevertheless, we observe that L-shaped dams give rise to an increase of both Δh_{max} and U, while the mutual difference between north- and south-oriented bars is quite small (in accordance with Figures 4 and 6). T-shaped dams give an even larger increase of Δh_{max} and U, in accordance with Figure 8 (as a T-dam can be considered as a combination of two L-shaped dams), and the largest increase is found again for Y-shaped dams, in accordance with Figure 10. It is noteworthy that the relative increase of U is always smaller than the relative increase of Δh_{max} and also exhibit less pronounced peaks in Figure 15. This can be explained by the fact that, according to the Q-H curves denoted by Equations (8)–(12), velocity U and discharge q through a barrier always approximately vary with the square root of Δh.

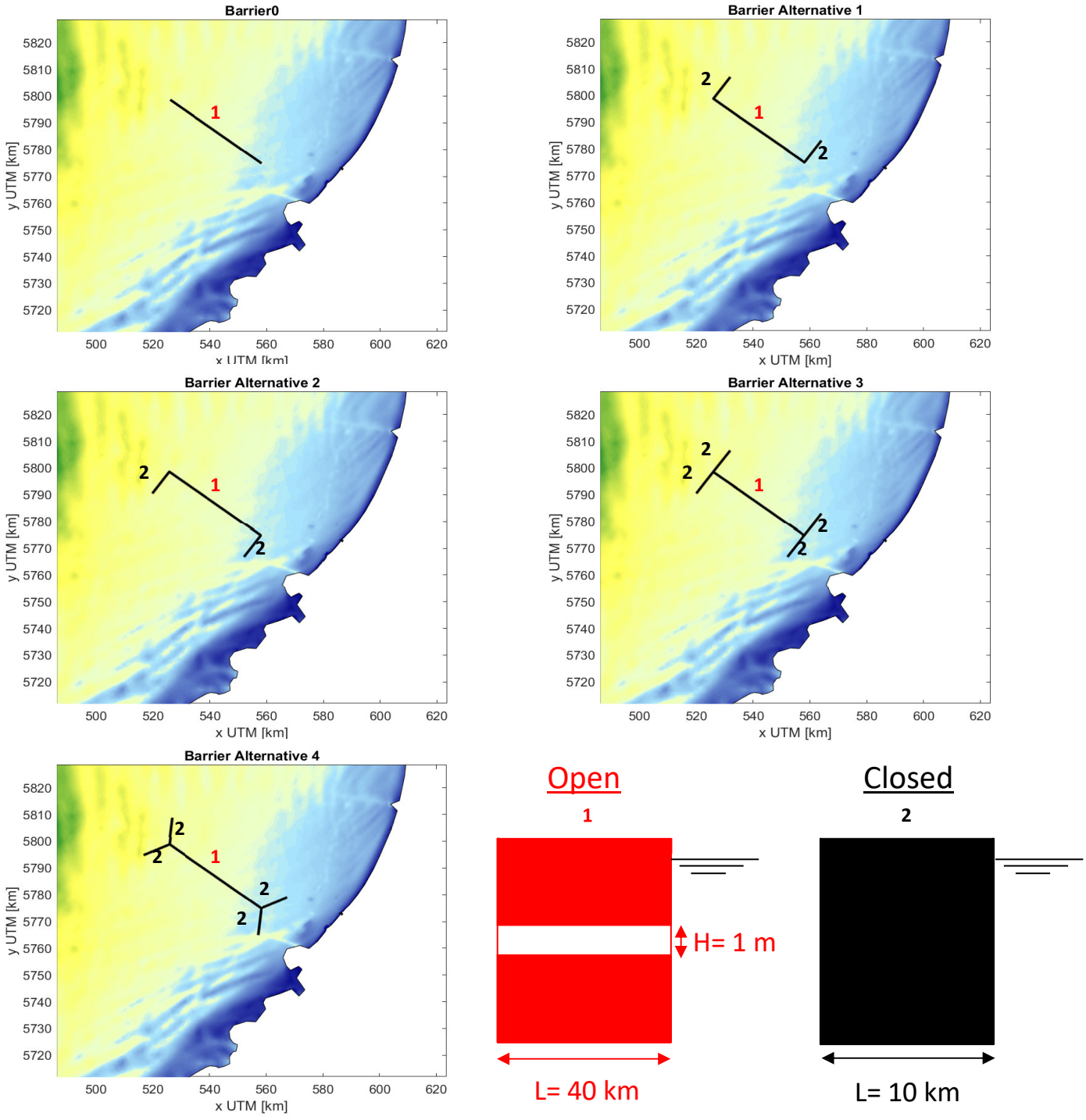

Figure 14: Reference DTP barrier 0 near Hoek van Holland (L = 40 km), with optional L-, T- and Y-shaped bars.

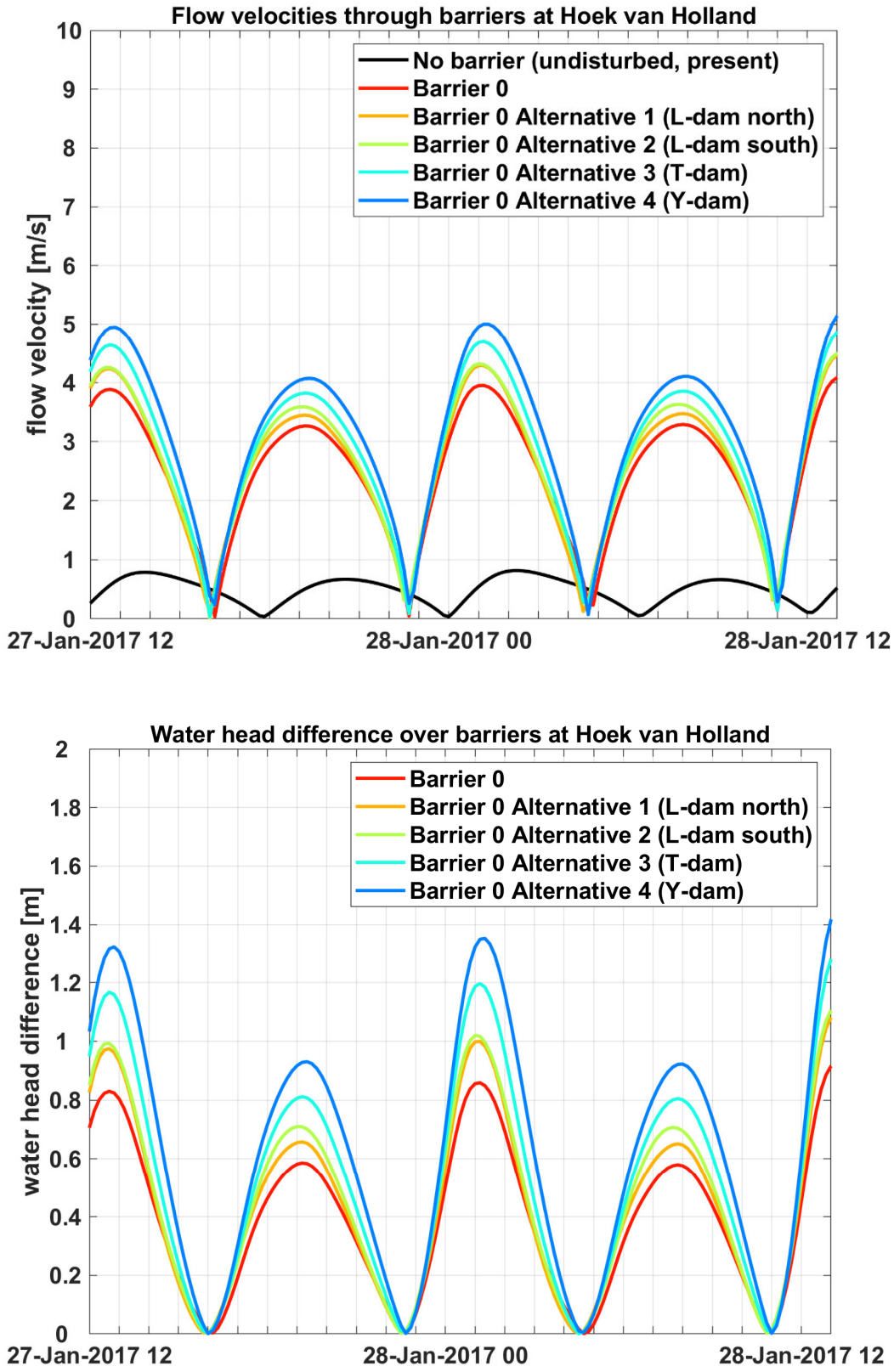

Figure 15: Maximum flow velocity perpendicular to DTP barrier (upper panel) and maximum head difference across the barrier (lower panel) as a function of time, for reference case Barrier 0 (L = 40 km) with optional L-, T- and Y-shaped bars.

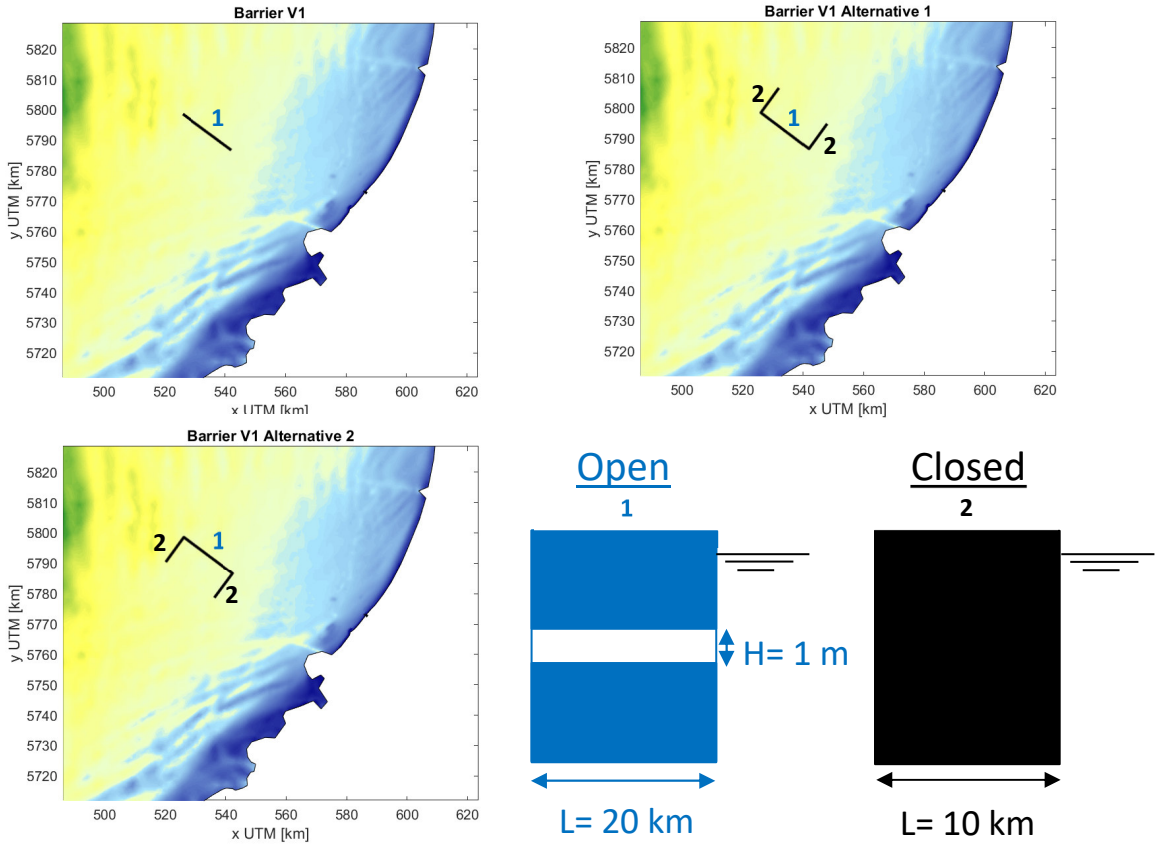

Figure 16: Shortened DTP barrier (V1) near Hoek van Holland (L = 20 km), with optional L-shaped bars.

Additional to the reference case Barrier 0, we also consider a shortened DTP dike of only 20 km length (coined Barrier V1), with possibly additional L-shaped bars. Figure 16 depicts the different alternatives that have been considered, in accordance with the schematized design alternatives addressed before in the Figures 1–6 and 14-15. As shown in Figure 16, all possible bar extensions to the main DTP dike have equal length of 10 km and are fully watertight (H = 0.0 m).

In accordance with Figures 1–6, Figure 17 shows that both the maximum head difference and maximum velocity through the barrier (and hence the maximum discharge) increase for the subsequent alternatives that are considered. Because of the great influence of tidal asymmetry in the North Sea situation, no attempt is made here to "fit" the found results exactly into the framework of Equation (4). Nevertheless, we observe that L-shaped dams give rise to an increase of both Δh_{max} and U, while the mutual difference between north- and south-oriented bars is quite small (in accordance with Figures 4 and 6). It is noteworthy that the relative increase of U is always smaller than the relative increase of Δh_{max} ans also exhibit less pronounced peaks in Figure 17. This can be explained by the fact that, according to the Q-H curves denoted by Equations (8)–(12), velocity U and discharge q through a barrier always approximately vary with the square root of Δh. Finally, we observe that the maximum head differences found in Figure 17 are approximately 50% of those found in Figure 15, while Barrier V1 has 50% of the length of Barrier 0. This implies that, even in case of dominant tidal asymmetry, one can still argue that the head difference Δh_{max} is still roughly proportional to the DTP dam length, as anticipated by Equations (3) and (7).

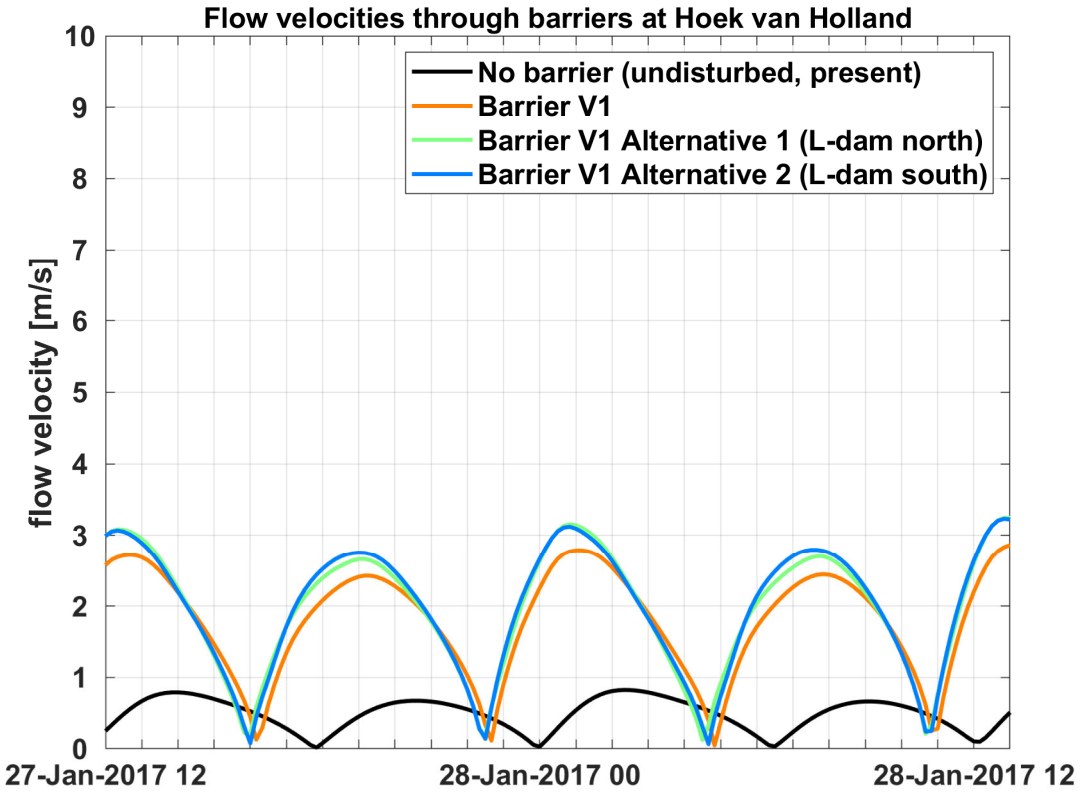

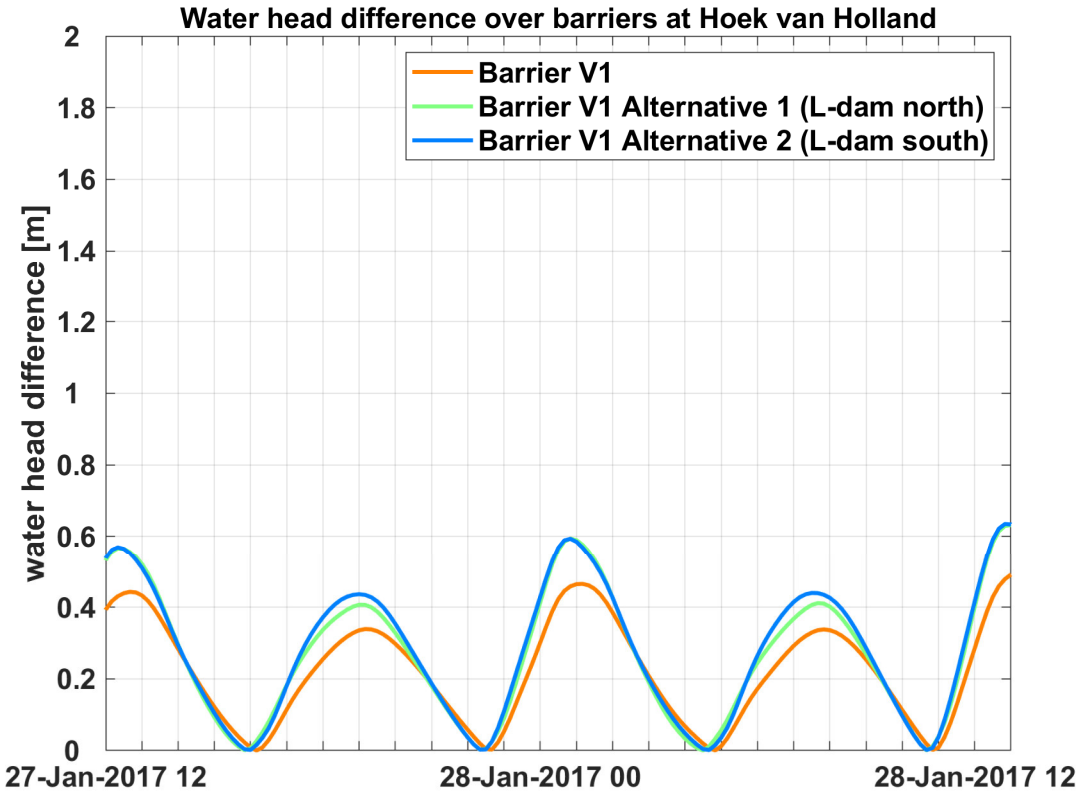

Figure 17: Maximum flow velocity perpendicular to DTP barrier (upper panel) and maximum head difference across the barrier (lower panel) as a function of time, for shortened DTP barrier (V1) (L = 20 km) with optional L-shaped bars.

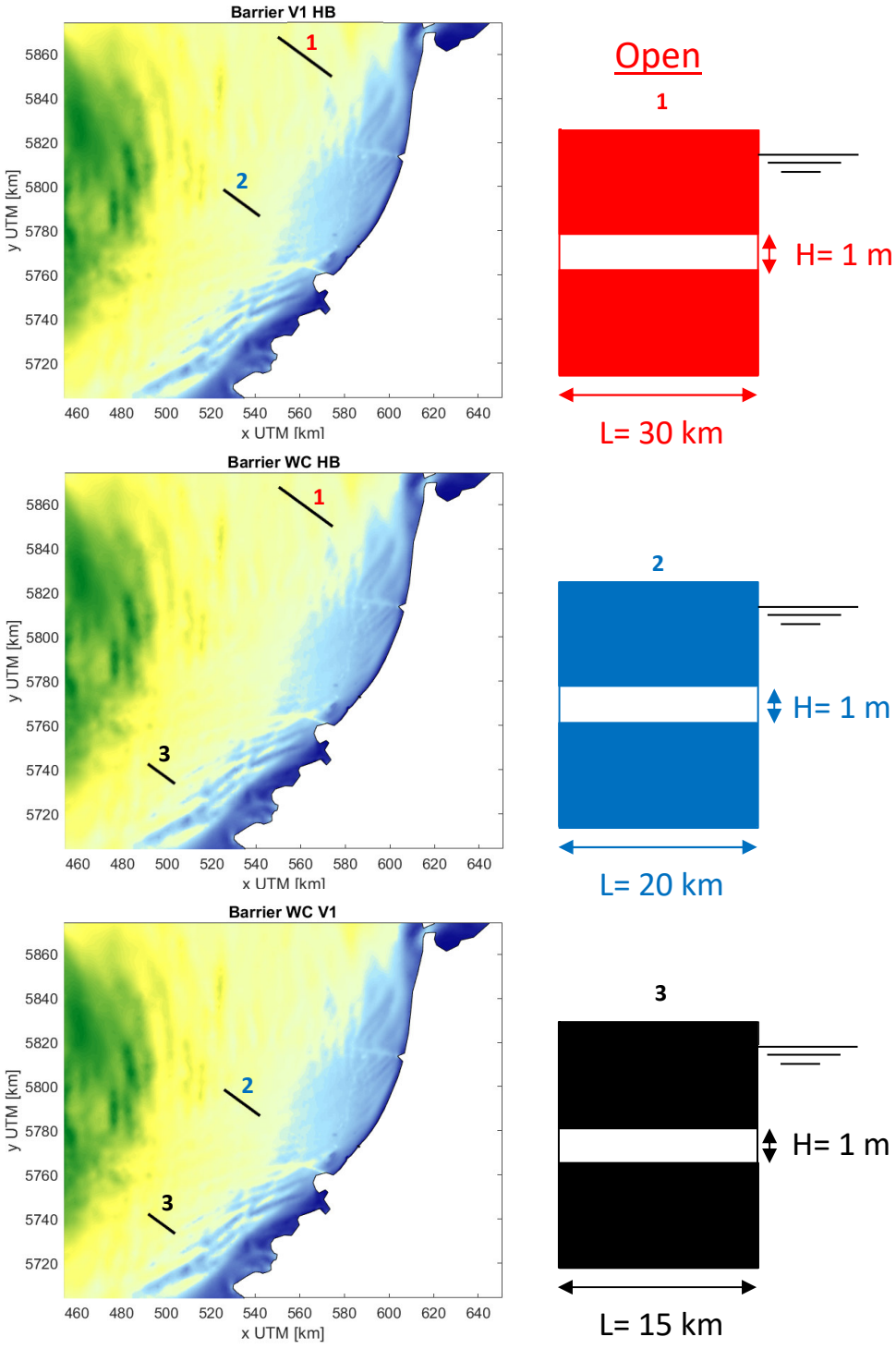

Figure 18: Three different combinations of two (out of three) DTP barriers of 30 km, 20 km and 15 km respectively. Abbreviations: HB = Hondsbossche, V1 = Hoek van Holland barrier case shown in Figure 16, WC = Walcheren. All three barriers have gate height H = 1.0 m.

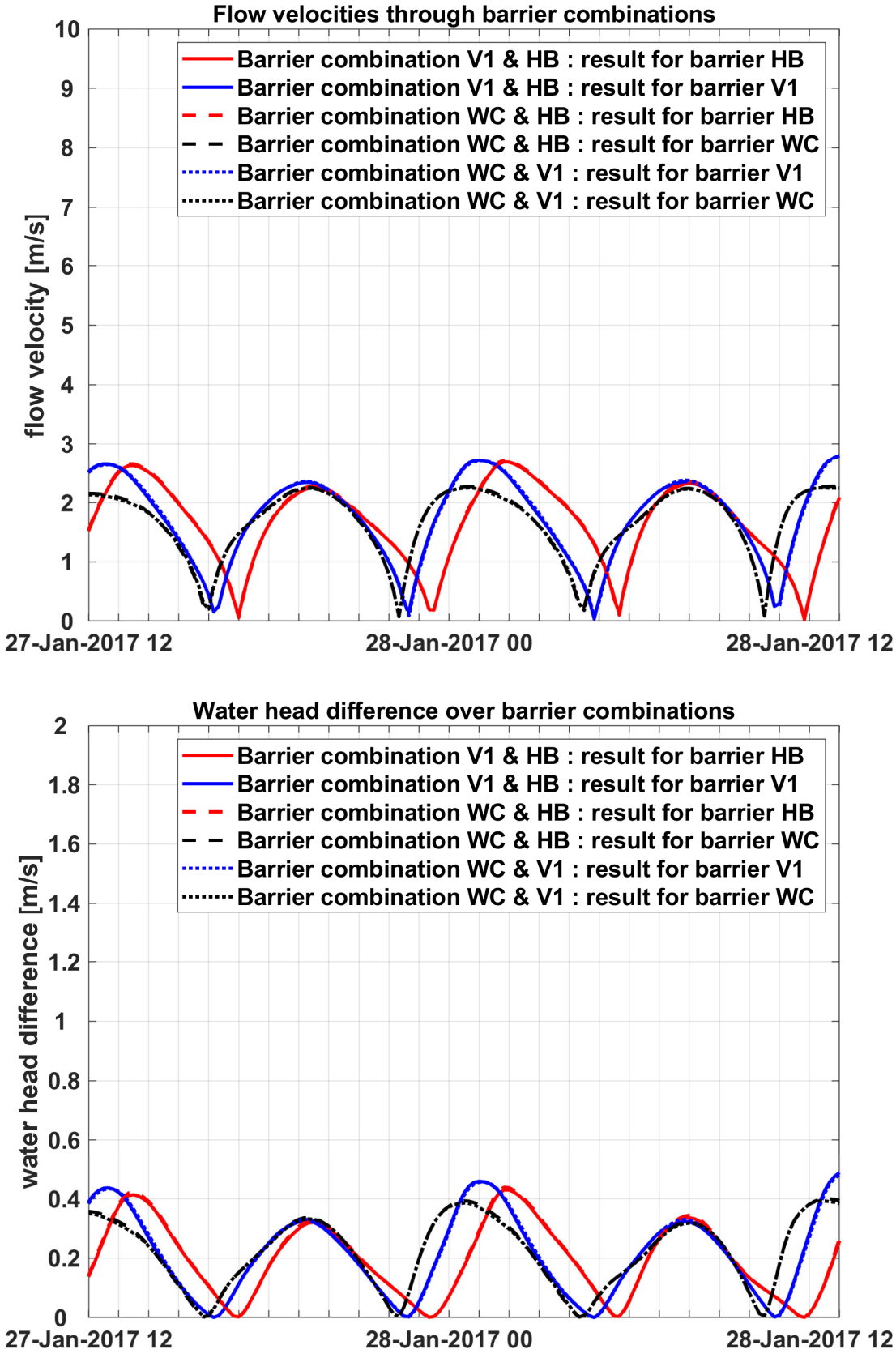

Figure 19: Maximum flow velocity perpendicular to DTP barrier (upper panel) and maximum head difference across the barrier (lower panel) as a function of time, for three combinations of two (out of three) DTP barriers along the Dutch coast.

It has been proposed by various authors that two or more combined DTP dams could be advantageous for the creation of a constant and reliable baseload. For instance, if two DTP dams are constructed at such a distance from each other that their ambient tidal flow is approximately 3 hours out of phase (close to one quarter of an average tidal period), the one dam will be functioning and generate tidal power at full flood/ebb while the other dam experiences slack water and is therfore temporarily idle.
In view of this option, we here consider a number of combinations of DTP dams along the Dutch coast. Three dams are projected: the shorter Hoek van Holland dike treated before ("V1", 20 km), a dike off-shore near Hondsbossche ("HB", 30 km) and a dike off-shore near Walcheren ("WC" 15 km). Three simulations have been performed, in which two out of three dams were combined each time. No L-, T- or Y-shaped extensions are considered here. We are especially interested in the possible mutual influence of these dams with respect to the values of Δh_{max} and U they experience. Figure 18 depicts the different alternatives that have been considered.

Figure 19 shows the maximum head difference and maximum velocity through the barrier for all of these double-DTP dam combinations; obviously, we consider the hydrodynamic effect of each combination on *both* dams. For each combination, the resulting maximum Δh_{max} and U values are quite comparable for Hondsbossche (HB) and Hoek van Holland (V1); the Δh_{max} and U values found for Walcheren (WC) are slightly below this level due to the fact that this dam is significantly shorter. (Although the HB dam is longest by far, the local tidal range is smallest there because it is rather close to the amphidromic point in the southern North Sea, which compensates the difference with the V1 dam that would have resulted otherwise.)
It is striking that, in each panel of Figure 19, the six plotted lines are actually bundled in three groups of two lines. For instance, we observe that both results for the Hondsbossche dam are virtually equal, regardles whether this HB dam is combined with V1 or WC. The same result holds for the other two dams, and in holds for both Δh_{max} and U. From this result we conclude that the three dams depicted in Figure 18 are actually hydrodynamically independent (!); their mutual influence is negligible.
This can be explained by the fact that these dams are relatively short compared to the tidal wave length (and short compared to the 40-km reference dam Barrier 0 and most DTP dikes treated in Section 3), so that tidal diffraction does not play a dominant role in this case. Only diffraction and reflection effects would be able to account for the mutual influence of these three dikes, whereas the three cases considered here appear to answer rather well to the basic local added-mass theory outlined in Section 3 (apart from the fact that tidal asymmetry remains important at all times).

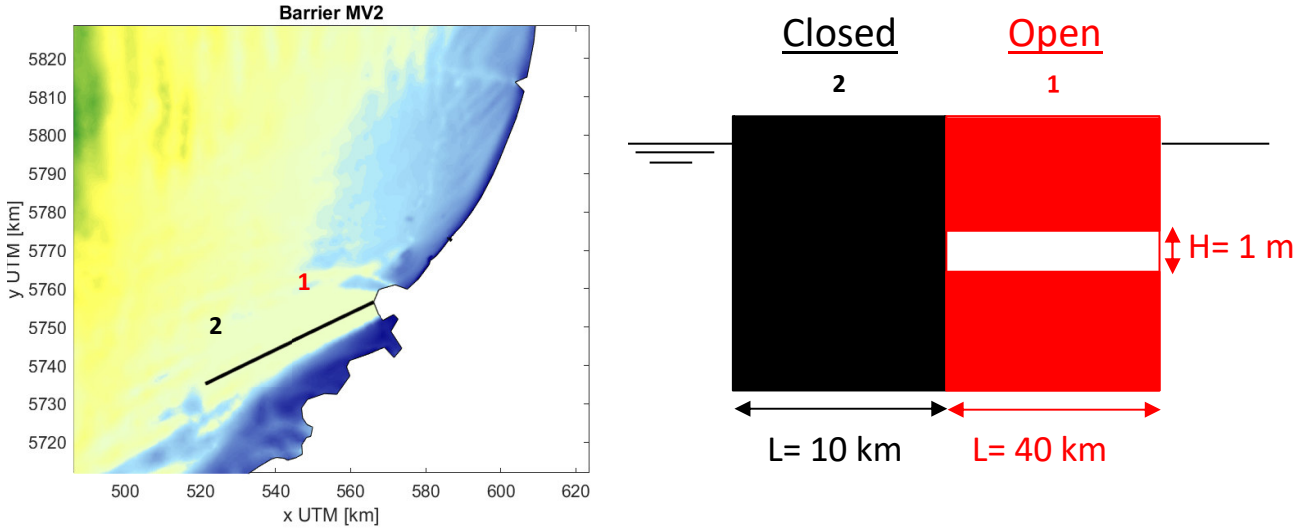

Figure 20: DTP barrier configuration at Maasvlakte II (length 50 km, of which 40 km permeable and 10 km closed).

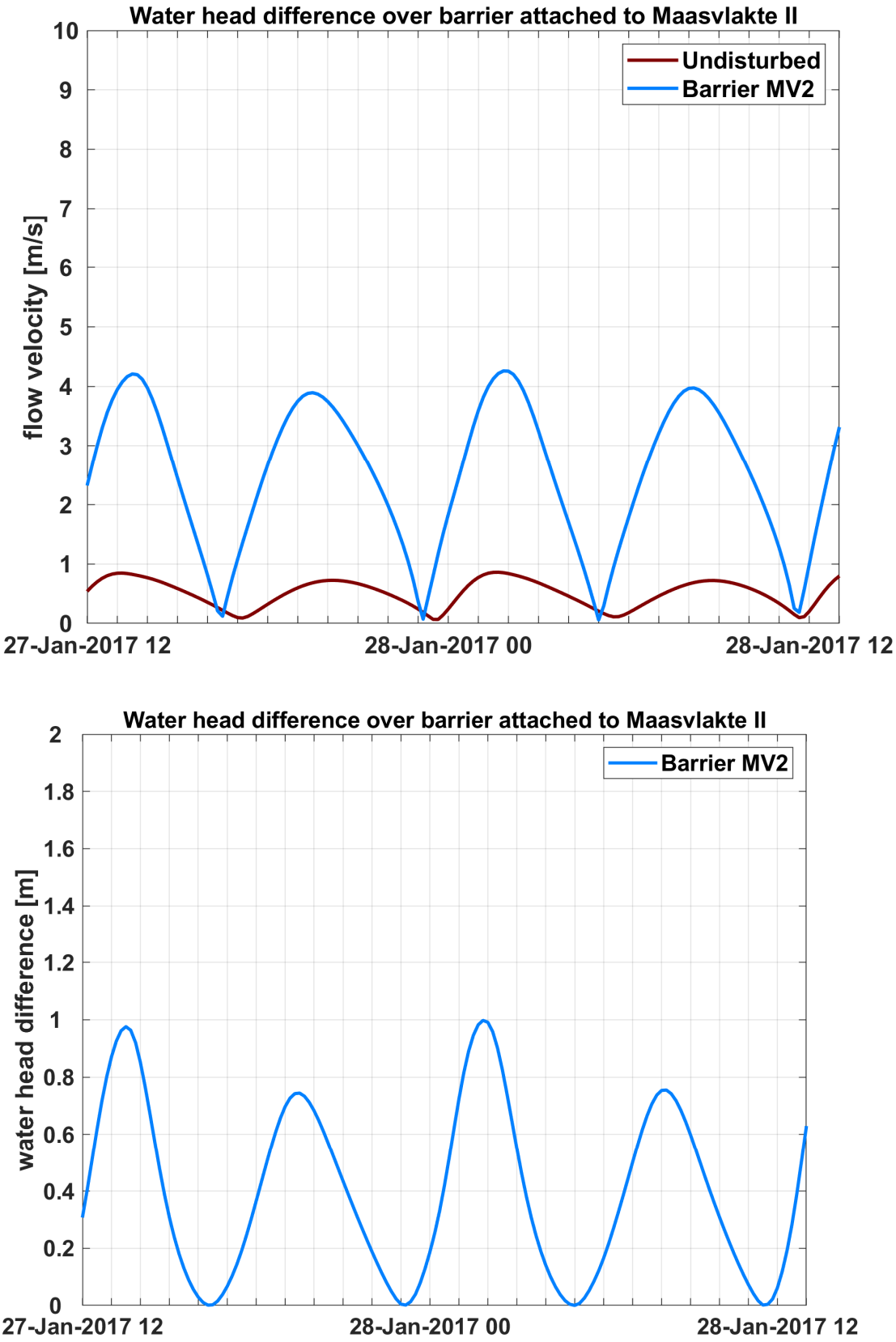

Figure 21: Maximum flow velocity perpendicular to DTP barrier (upper panel) and maximum head difference across the barrier (lower panel) as a function of time, for the DTP barrier configuration attached to Maasvlakte II.

To conclude this section, we finally consider the practical case which is shown in Figure 20: a DTP dike of length 50 km connected to the Dutch coast, which comes ashore at the location of the recent Maasvlakte II land reclamation. Among all possible coast-connected DTP alternatives that could be proposed this option seems especially worthwhile, for several reasons:

- As the DTP dike is connected to an already seaward-pointing industrial area (instead of a beach or coastal area that is valuable in terms of ecology, recreation or otherwise), the solution presented here might be more acceptable for the great amount of stakeholders involved in the coastal region;
- Directly south of the seaward-pointing Maasvlakte II a tidal basin can be formed which is confined westward by the DTP dike and fully opened southward, which offers ample possibiliy to create a considerable head difference and lateral discharge on behalf of DTP, while important navigation routes for trade and fishing are basically not blocked.

Figure 20 depicts a straight dike of 50 km length, of which the seaward end is fully watertight over length 10 km and the remaining part is partially open over length 40 km (with H = 1.0 m). It is anticipated that the seaward end of the dike will experience hardly any head difference in this case, whereas the maximum head difference can be expected near the coast of Maasvlakte II. In the present case, it would probably be very counter-productive to add any L-, T- or Y-shaped bar to the DTP dike, as these additions would block the tidal flow in a quite disadvantageous way. However, it remains possible to replace the present straight dike by a curved dike bending gradually southward, in order to "catch" more tidal area (added mass!) and in order to streamline the tidal flow outside the DTP basin in such a way to reduce possible drag.

Figure 21 shows the maximum head difference and maximum velocity through this barrier attached to Maasvlakte II. Although this Figure itself offers no other data for mutual comparison, it is possible to make a comparison with the Figures 15 and 17, which show the 40-km and 20-km Hoek van Holland barrier results. We observe that, even though the Maasvlakte-II barrier is considerably heading southward along the coast (instead of westward blocking the tidal flow), still a remarkable head difference Δh_{max} and normal velocity U are achieved. This is due to the fact that the "DTP basin" along the Delta coast of Zeeland is advantageously exposed toward the usual tidal wave that enters the basin from the southwest. Moreover, thanks to the basin length of approximately 50 km, a certain amount of tidal resonance results east of the DTP dike which considerably enhances the tidal head difference across the dike.

This scenario is especially attractive because:

- This advantageous head difference hardly comes at the cost of any considerable disturbance of the tidal wave at open sea (and potentially inconvenient shifts of amphidromic points resulting from it);
- Because DTP dikes attached to a coastline are efficient and attractive in terms of power output in any case; and
- Because hardly any navigation routes are blocked, and existing coastal communities or ecosystems are disturbed as least as possible.

Summarizing: the practical Dutch North Sea coast results shown in this section indicate that the basic trends and proportionalities of DTP hydrodynamics, as shown before in Section 3 for a schematized case, are also present in a modelled real-life environment. Such as:

- The (approximate) proportionality of maximum head difference with dam length;
- The very important role of tidal asymmetry and drag forces, which limit the applicability of the basic Equation (3) for Δh_{max};
- The impact of adding L-, T- or Y-shaped bars to straight DTP dikes;
- Locality of the hydrodynamic impact of "twin dams" that are not too long and sufficiently distant from each other, so that their diffraction patterns do not interfere;
- Influence of partial dike permeability on flow velocity, head difference and phase shift.

Besides these basic trends, the influence of complex topography such as coastlines, bed friction and bathymetry is of course also present within these North Sea results.

7 DISCUSSION AND CONCLUSIONS

In this memorandum we have reviewed the basic principles of the Dynamic Tidal Power (DTP) technique, giving an overview of existing literature on the hydrodynamic aspects of it, and elaborating these principles in two series of numerical calculations: a schematized rectangular sea (Section 3) and the Dutch North Sea coast (Section 6).
Both series of numerical models show basic trends and proportionalities that are characteristic for DTP hydrodynamics, such as:

- Proportionality of maximum head difference with dam length;
- The important role of tidal asymmetry and drag forces;
- The positive impact of adding L-, T- or Y-shaped bars to straight DTP dikes;
- Locality of the hydrodynamic impact of “twin dams” that are not too long and sufficiently distant from each other;
- Influence of partial dike permeability on flow velocity, head difference and phase shift.

It is concluded that numerical simulations are an indispensable tool for assessing the hydrodynamic effects and power output o a DTP dike, even for the simplest schematized cases; this conclusion can be attributed to the fundamental importance of non-linearities in most tidal flows with a realistic amplitude or tidal range (of order 1-2 m). As indicated by Dai et al. (2018) and Section 3 in this study, the presence of tidal asymmetry and drag makes the prediction of the water head difference over a DTP dike very location-specific. Moreover, for many of the dike lengths considered, tidal diffraction around a DTP dike gives rise already to deviations from the basic theory as given by Hulsbergen et al. (2005, 2008), Bitter (2018) and Mei (2012, 2019, 2020) in Equations (3) and (7). This means that, even in idealized cases without complex topography, the linear theory as presented by these authors yields only indicatory results; the empiric deviation factor of 1.7 as found for the practical IJmuiden case by Hulsbergen et al. (2008) forms an indicator for this already. Obviously, in practical DTP cases many complex topographical influences will be present as well, such as bathymetry, bed friction, Coriolis force, coastlines and tidal spectra consisting of many different components.
Although it is clear that the basic hydrodynamic principle behind DTP certainly “works”, it is also clear that it is often not possible to pin this principle down upon one single or simple formula, as simply too many geometrical complexities and hydrodynamic non-linearities are involved.

With respect to the relation between water head difference and discharge through DTP turbines, we note that the Q-H curves and energy output relations as applied in literature seem to have quite a preliminary character. For instance, the Q-H curves as presented by Bitter (2018) and Mei (2019, 2020) have a mathematical shape that is rather different, and sometimes potentially confusing as far as the physical meaning of the various discharge coefficients and energy efficiency coefficients is concerned. Therefore, in this memorandum we review the basic physical principles of energy harvest by DTP turbines but we do not “promise” certain energy output levels, like has been done before elsewhere (see Bitter 2018, Mei 2020).
We conclude that there is actually still a great lack of data with respect to the design specifications of “realistic” energy turbines suitable for DTP; estimates of their real Q-H curves and real energy efficiencies seem to differ considerably throughout literature. Filling this knowledge gap, possibly experimentally on prototype scale, is still an important research step to be taken. Finally, we conclude that it is vital to fit parameterizations of energy turbines into a larger-scale numerical model in order to achieve a true dynamical coupling between water head difference and discharge through a dam.

A hydrodynamic issue that still awaits further research is the question what influence a specific DTP dike configuration will have on the tidal pattern of the surrounding marine environment. Results from Section 3 and 6 suggest that the hydraulic impact of a DTP dike remains virtually local for short dams. However, will a larger dam configuration be able to cause a shift in the tidal pattern of e.g. the North Sea, such as the locations of amphidromic points? If this would be the case, it would also cause a shift in the usual tidal ranges that can be expected along the North Sea

coast (also internationally), which may cause great inconveniences along this entire coastal area (e.g. beach erosion, drying and wetting of ecologically important tidal flats, increased need for harbour dredging or shore protection).

Another aspect to be investigated further regards the morphological impact of DTP dikes, both locally and globally.
In terms of local impact, we anticipate that alternate regions of erosion and deposition will develop along the DTP installation. Beyond the open-sea end points of a DTP dike (or, likewise, its T- or Y-bars), regions of bed erosion are expected due to the locally enhanced flow velocity; also local drag effects may occur, which cause large-scale eddies in the dike's wake region and/or spiral flow along the dike tip (quite similar to the situation of river groynes). On the other hand, along both long sides of the DTP dike the local velocity will obviously decrease due to flow stagnation, which may give rise to local deposition of sediment. This deposition effect is likely to threaten the functionality of locally present DTP turbines, whereas the erosion effect along the dike tips may threaten the over-all stalibity of the installation.
In terms of global impact, the initial sedimentation-erosion pattern sketched above may give rise to a shift of the over-all tidal flow pattern at sea in the long run, which compromises the functionality of the DTP dam in yet another way. It is recommended to investigate whether DTP dikes could be installed at open sea on locations which are not too "active" morphologically.
Especially the case of DTP dams attached to a morphologically active alluvial coast is important. It is known that "hard" structures such as long breakwaters perpendicular to the coast may interrupt the longshore transport of sediment, which acts as a vital "conveyor belt" of sand that ensures coastal stability. An interruption of this longshore sediment transport by a coastal DTP installation could disrupt coastal equilibrium which may have strong consequences on the "downdrift" side of the dam, such as beach and dune erosion even at long distance of the dam or an increase of the well-known "sand hunger" of the Wadden Sea.

We conclude the discussion on hydrodynamics by a few remarks about the reliability and constantness of the envisioned sustainable energy baseload.

On the one hand, the functionality of a DTP installation on a daily basis is virtually guaranteed due to the permanent presence of solar and lunar tidal influence on earth. This tidal influence is available along the entire earth's ocean surface and will not vanish in the very long run. The presence of two daily high-water peaks and two low-water troughs in the North Sea implies the occurrence of four tidal velocity peaks virtually each day. The daily velocity fluctuation based on astronomical tide is highly predictable and, hence, if these four velocity peaks would be equal in size, the time-average need for energy storage to create a constant power baseload could be relatively low compared to wind and solar energy (which have a much more irregular and climate-dependent character).

However, there are still several factors which threaten the constancy of the DTP baseload to a great extent. First of all, twice each month the solar and lunar tide are 0° or 180° out of phase (spring tide, during New Moon or Full Moon) resp. 90° or 270° out of phase (neap tide, during First or Third Quarter of the Moon). Along the Dutch North Sea coast, the tidal range reduction due to neap tide versus spring tide can be typically 20-30%; this leads to a proportional reduction of the water head difference over DTP dikes, multiplied by a discharge through the turbines that is consequently reduced as well (!). Hence, a net power reduction of 50% twice a month is a rather realistic scenario. (The FINEL simulations shown in Section 6 have been run during spring tide.)

An inconvenient aspect of spring tide-neap tide cycli is that they occur over the entire earth's ocean surface simultaneously (!); hence, a DTP power fluctuation in the North Sea due to neap tide cannot be cured by buying energy from the Yellow Sea, for instance. All DTP installations in the world will suffer the same fluctuation. In order to neutralize this fluctuation, a range of measures could be taken: such as significantly increasing the long-term DTP energy storage capacity (after all), or otherwise allow the remaining existence of reliable (but not so sustainable) energy

baseloads like fossile or nuclear energy, to account for a DTP power deficit during neap tidal periods.

It is not aimed here to calculate the vast additional storage capacity needed for DTP to nivellate the spring-neap tidal cycle sketched above. However, it is anticipated that the big storage advantage of DTP compared to wind and solar energy will be at least compromised to some extent.

In a different fashion, a similar threat to baseload reliability is posed by wind influence at open sea. During north-west storm surge periods the mean sea water level in the southern North Sea can rise several meters, which may give rise to a slight damping of the tidal signal for a couple of days. But also outside storm conditions, at moderate wind speeds (say force 6 or 7 on Beaufort scale), wind may already affect the real-time tidal flow velocity along the Dutch coast. A lasting wind field from north or northwest direction may, for instance, partially block or withhold the tidal flood current (traveling north along the coast), whereas the ebb current (traveling south) is enhanced on the contrary. For a long-lasting southwestern wind field, the effect can be the other way round. This means that only two daily tidal velocity peaks remain instead of four (although these two peaks are higher as well), intercut by longer periods of weak flow conditions. Though the net effect of the power output could be limited, such meteorological conditions can give rise to need for more short-term energy storage capacity.

The above discussion on hydrodynamics will, of course, be accompanied by political discussion regarding e.g. feasibility, construction costs and side effects when it comes to the design and planning of a real DTP installation. As pointed out by Mei (2020), the construction of a new DTP dam will not only be very expensive but also will likely face strong environmental objections by coastal communities and stakeholders; therefore, a worthwhile alternative may be to find an existing cape or island which can account for part of the tidal flow blocking. A good example in the British situation could be the Weymouth peninsula along the English south coast (Dorset); to a certain extent, the Maasvlakte II land reclamation area may play a similar role in the Dutch situation (see Figures 20 and 21 in Section 6).

The eventual feasibility of DTP must, of course, await further studies on turbine specifications and economic, ecological or political impacts of the proposed technique. Especially the topic of international cooperation is of importance, not only due to cross-border effects of national DTP initiatives, but also due to the division of e.g. the North Sea into territorial waters and economically exclusive zones, offshore wind farms and fishing grounds.

Due to the very high cost level of prototype-scale experiments on DTP, it is recommendable to assess whether certain laboratory-scale or medium-scale experimental setups could add some value to the evaluation of the DTP technique. It should however be kept in mind that an important geophysical aspect of open-sea DTP flow like the Coriolis effect is essentially *not* scalable. On the other hand, yet, it is possible to represent long tidal waves on laboratory scale using Froude scaling. Testing a tidal energy turbine, however, is probably less worthwhile on laboratory scale due to the low Reynolds number; testing such a turbine could better take place on some medium scale at least, if not a prototype scale (using a single turbine).

REFERENCES

Ali, T., Gupta, S.D., Arnab, I.Z., Ferdous, S.M. (2012). An analysis of the potentiality of tidal power in Swandwip by using one- ad two-way power generation technology: an ideal model. *International Journal of Renewable Energy Research*, Vol. 2, No. 3, pp. 535-530, 2012.

Bitter, G., Antea Group (2018). Hydraulische vermogensrelaties en potentiebepaling DTP. In: Memorandum “Dynamic Tidal Power (DTP, Energie uit getijdenstromen in de Noordzee”, Humsterland Energie, 14 december 2018.

Buchwald, V.T. (1971). The diffraction of tides by a narrow channel. *Journal of Fluid Mechanics*, Volume 46, pp. 501-511, 1971.

Buchwald, V.T., Miles , J.W. (1974). Kelvin-wave diffraction by a gap. *Journal of the Australian Mathematical Society*, Volume 17, Issue 1, pp.29-34, 1974.

Dai, P., Zhang, J.S., Zheng, J.H., Hulsbergen, K., Van Banning, G., Adema, J., Tang, Z.X. (2018). Numerical study of hydrodynamic mechanism of dynamic tidal power. *Water Science and Engineering* 11(3), pp. 220-228, 2018.

Det Norske Veritas (2010). Offshore Standard DNV-OS-J101 – Design of Offshore Wind Turbine Structures, Report/Manual by Det Norske Veritas, October 2010.

Gaia Project / Projet Gaia (2014). Electricity Generation: Tidal and Wave Energy. An overview of electricity generated using tidal and wave energy. The Gaia Project, Fredericton, New Brunswick, Canada, 2014.

Hulsbergen, K., Steijn, R. Hassan, R., Klopman, G., Hurdle, D. (2005). Dynamic Tidal Power (DTP). *Proceedings of the 6th European Wave and Tidal Energy Conference (EWTEC)*, Glasgow, UK, August 29 – September 2, 2005, pp. 217-222.

Hulsbergen, K., Steijn, R., Van Banning, G., Klopman, G., Fröhlich, A. (2008). Dynamic Tidal Power (DTP) – A new approach to exploit tides. *Proceedings of the 2nd International Conference on Ocean Energy (ICOE)*, Brest, France, 2008, pp. 1-10.

Hulsbergen, K. (2012). Dynamic Tidal Power for Korea. *Proceedings of the 1 st Asian Wave and Tidal Conference Series (AWTEC), 2012.*

Labeur, R.J. (2009). Finite element modelling of transport and non-hydrostatic flow in environmental fluid mechanics. *Ph.D. Thesis*, Delft University of Technology, Delft.

Labeur, R.J., Wells, G.N. (2012). Energy stable and momentum conservative interface stabilised Finite Element Method for the incompressible Navier-Stokes equations. *SIAM Journal on Scientific Computing*, 34(2), A889-A913.

Lemmens, C. (2017). Modeling the extraction of tidal energy from the hypothetical Orkney Islands Dam (northern North Sea) and from turbines in a tidal inlet. *M.Sc. thesis*, Utrecht University, July 15, 2017.

Liu, Q., Zhang, Y. (2014). Hydrodynamic stuy of phase-shift tidal power system with Y-shaped dams. *Journal of Hydraulic Research*, Volume 52, No. 3, pp. 356-365, 2014.

Mei, C.C. (2012). Note on tidal diffraction by a coastal barrier. *Applied Ocean Research* 36, pp. 22-25, 2012.

Mei, C.C. (2019). Quick estimates of power output through a DTP dam. Memorandum to ir. W.L. Walraven, Stichting Middag Humsterland Duurzaam, September 15, 2019.

Mei, C.C. (2020). Tidal diffraction by a small island or cape, and tidal power from a coastal barrier. *Journal of Fluid Mechanics*, Volume 897-A13, pp. 1-24, 2020.

Roy, P., Das, R., Topu, S.H. (2015). Possibilities of Tidal Power in Bangladesh. *Proceedings of the International Conference on Mechanical Engineering* (ICME), Dhaka, Bangladesh, December 18 – 20, 2015.